Since January 2020 Elsevier has created a COVID-19 resource centre with free information in English and Mandarin on the novel coronavirus COVID-19. The COVID-19 resource centre is hosted on Elsevier Connect, the company's public news and information website.

Trends in Analytical Chemistry 143 (2021) 116342

Contents lists available at ScienceDirect

Trends in Analytical Chemistry

journal homepage: www.elsevier.com/locate/trac

Applications of scaffold-based advanced materials in biomedical sensing

Roya Sarkhosh-Inanlou [a, b, 1], Vahid Shafiei-Irannejad [a, 1], Sajjad Azizi [b], Abolghasem Jouyban [c, d], Jafar Ezzati-Nazhad Dolatabadi [e], Ahmad Mobed [f], Bashir Adel [g, h], Jafar Soleymani [c, **], Michael R. Hamblin [i, *]

[a] Cellular and Molecular Research Center, Cellular and Molecular Medicine Institute, Urmia University of Medical Sciences, Urmia, Iran
[b] Biotechnology Research Center, Tabriz University of Medical Sciences, Tabriz, Iran
[c] Pharmaceutical Analysis Research Center, Tabriz University of Medical Sciences, Tabriz, Iran
[d] Immunology Research Center, Tabriz University of Medical Sciences, Tabriz, Iran
[e] Drug Applied Research Center, Tabriz University of Medical Sciences, Tabriz, Iran
[f] Aging Research Institute, Faculty of Medicine, Tabriz University of Medical Sciences, Iran
[g] Food and Drug Safety Research Center, Tabriz University of Medical Sciences, Tabriz, Iran
[h] Liver and Gastrointestinal Diseases Research Center, Tabriz University of Medical Sciences, Tabriz, Iran
[i] Laser Research Centre, Faculty of Health Science, University of Johannesburg, Doornfontein, Johannesburg, 2028, South Africa

ARTICLE INFO

Article history:
Available online 21 May 2021

Keywords:
Biomedical sensing
Advanced materials
Scaffold materials
Infectious diseases
Disease biomarkers
Severe acute respiratory syndrome coronavirus

ABSTRACT

There have been many efforts to synthesize advanced materials that are capable of real-time specific recognition of a molecular target, and allow the quantification of a variety of biomolecules. Scaffold materials have a porous structure, with a high surface area and their intrinsic nanocavities can accommodate cells and macromolecules. The three-dimensional structure (3D) of scaffolds serves not only as a fibrous structure for cell adhesion and growth in tissue engineering, but can also provide the controlled release of drugs and other molecules for biomedical applications. There has been a limited number of reports on the use of scaffold materials in biomedical sensing applications. This review highlights the potential of scaffold materials in the improvement of sensing platforms and summarizes the progress in the application of novel scaffold-based materials as sensor, and discusses their advantages and limitations. Furthermore, the influence of the scaffold materials on the monitoring of infectious diseases such as severe acute respiratory syndrome coronavirus 2 (SARS-CoV-2) and bacterial infections, was reviewed.

1. Introduction

The early detection of diseases, particularly cancer is an important goal of the biomedical community. Early detection of diseases provides a chance of a successful treatment and reduces the overall cost of the therapeutic procedure. The early stage diagnosis of diseases requires the development of effective and reliable analytical systems for the identification and quantification of disease biomarkers present in different biological fluids such as whole blood, plasma, serum, urine, etc. [1].

Infectious diseases are particularly suited to analysis by these devices, which can rapidly detect disease markers with high accuracy. The current pandemic of severe acute respiratory syndrome coronavirus (COVID 19) underlines the importance of early and rapid detection approaches. A reliable detections system could reduce COVID 19 mortality.

The synthesis of novel advanced materials can be important for the development of analytical methods for biomarker detection. Scaffold-based materials can be utilized in these advanced systems due to their superior physicochemical properties and relatively easy surface functionalization [2,3].

Scaffold-based materials are three-dimensional (3D) substances, which serve an important role in the reconstruction of a range of anatomical defects that can occur in tissues. The porous nature of these materials allows the passage of biological fluids, and enhances cellular activities such as adhesion, proliferation,

* Corresponding author.
** Corresponding author.
E-mail addresses: jsoleymanii@gmail.com, soleymanij@tbzmed.ac.ir (J. Soleymani), hamblin.lab@gmail.com (M.R. Hamblin).
[1] Equality contributed.

https://doi.org/10.1016/j.trac.2021.116342
0165-9936/

Abbreviations

POEGMA	Oligo (ethylene glycol) methacrylate
HEA-TDI	2-(Acryloxy)ethyl (3-isocyanato-4-methylphenyl) carbamate
BTP	2,5-Bis(benzo[d]thiazol-2-yl)
APBA	3-Aminophenylboronic acid
CdS-QDs	Cadmium sulfide-quantum dots
CDHA	Calcium deficient hydroxyapatite
CDs	Carbon dots
PVA	Poly (vinyl alcohol)
CHI	Chitosan
ChA	Chronoamperometric
COFs	Covalent organic frameworks
CNC	Cellulose nanocrystal
CV	Cyclic voltammetry
DPV	Differential pulse voltammetry
DzW	DNAzyme walker
EIS	Electrochemical impedance spectroscopy
ECL	Electrochemiluminescence
ECH	Electroconductive hydrogel
GA	Glutaraldehyde
AuAC−CoO	Gold atomic cluster−cobalt oxide
AuNCs	Gold nanoclusters
HRP	Horseradish peroxidase
HA NPs	Hydroxyapatite nanoparticles
IC	Iminocoumarin
ITO	Indium tin oxide
LOD	Limit of detection
L-Au NPs	Luminol labeled gold nanoparticles
MSM	Mesoporous silica microspheres
MSNs	Mesoporous silica nanoparticles
MOF	Metal organic frameworks
MWCNT	Multiwalled carbon nanotubes
NPG	Nanoporous gold
NIR	Near-infrared
NG	Nitrogen-doped graphene
PEC	Photoelectrochemical
P4VP	Poly(4-vinylpyridine)
PA-DS	Poly-(allylamine)/dodecyl sulfate
PDMS	Polydimethylsiloxane
PEG	Polyethylene glycol
QG	Q Graphene
SPR	Surface Plasmon resonance
SERS	Surface-enhanced Raman spectroscopy
TSPP	Tetra(4-sulfonatophenyl) porphine dihydrochloride
TDN	Tetrahedron
YTDS	Y-shaped backbone-rigidified triangular DNA scaffold

migration and differentiation. These materials are designed to show low levels of toxicity and inflammation in tissues and organs [4].

Scaffolds can be generally categorized as ceramics [5], molecular [6–8], nanofiber [9], polymers [10], metal alloys [11,12], or composites [13] based on the type of compounds or materials that have been used in their construction. Scheme 1 illustrates some important scaffold-based materials. In addition, scaffolds can be classified as either natural or alloplastic materials, and degradable or non-degradable. Each type of scaffold displays its own physical, chemical, and mechanical properties, characterized by different pore sizes, functional groups, and morphology [14].

Recently, novel biomaterial scaffolds with low cytotoxicity, the ability to stimulate cell proliferation, and which have the advantage of being able to be printed in the laboratory, have received attention in biomedical science [15]. Different modifications such as, the introduction of surface functional groups, adjustment of the charge (negative or positive), tailoring of the hydrophobicity or hydrophilicity, and the flexibility or rigidity can be carried out on the scaffold materials to regulate their physicochemical properties and biological efficacy.

Scaffolds-based materials have been used in tissue engineering, and for the controlled release and delivery of drugs and other biomolecules like proteins or genes. These materials provide some important chemical and structural advantageous, including high porosity (useful for drug delivery, and production of light structures), abundant functional groups (which are needed for secondary surface modification), good biodegradability, and biocompatibility (which are required in tissue engineering for cell seeding and proliferation), high toughness and absorption capacity, good mechanical strength, etc. [16–18]. It is also noteworthy that all the physicochemical properties can be tailored according to the demands of the application. Apart from the advantages, some scaffold-based materials have limitations such as release of the material constituents, low mechanical strength, and in the fabrication of some scaffold-based materials, toxic materials i.e. hydrofluoric acid may be needed [11]. Various technologies have been employed to produce scaffolds with good biocompatibility and porosity to allow tissue regeneration and to simultaneously deliver biomolecules to the targeted tissue. Besides the applications of scaffold materials in tissue engineering and drug delivery [16,19], they have also been used in biosensing, which is the topic of this review. Despite the many applications of scaffold materials in tissue engineering, their applications in biosensing have been limited. Although their 3D structure can enhance the sensitivity of the biosensors approaches, their physicochemical properties may restrict their use in aqueous and biological media.

Scaffold-based materials have been reported for various biomedical applications over the years. An increasing trend can be observed from 1994 to 2019, underlining the importance of scaffold-based materials. Moreover, there is also an obvious increasing trend in the use of scaffold-based materials in biosensing. Scaffolds or nano-scaffold-based materials have mostly been employed for the detection and quantification of analytes, such as cancer biomarkers [3,20], glucose [21–23], pharmaceutical compounds [24–26], hydrogen peroxide [27], neurotransmitters [28–30], amino acids [31,32], or inorganic ions [33].

In the present review the applications of scaffold-based materials (alone or as hybrids) in biomedical sensing are discussed in detail. Various detection techniques have been utilized to detect different analytes in biological media. In this review, the analytical performance of each method is discussed and compared in order to identify the best approach for the detection of each analyte. Furthermore, the mechanism of action of each approach is explained. In addition, the application of scaffold-based materials in infectious disease detection is explored in a special section.

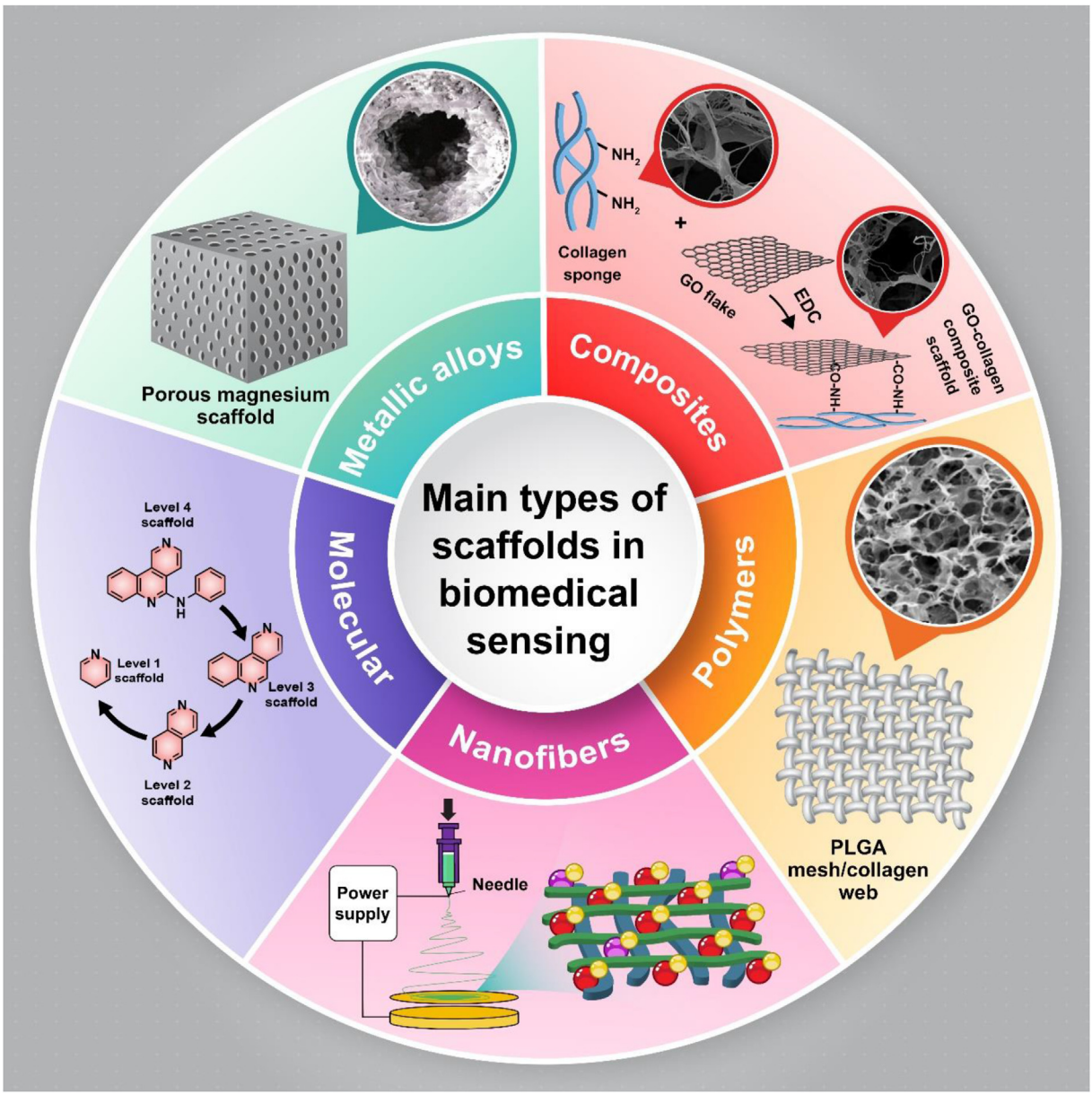

Scheme 1. Types of scaffolded materials.

2. Scaffold-based materials in biosensing for infectious disease and cancer diagnosis

2.1. Diagnosis of infectious disease

Outbreaks of infectious diseases are one of the major global health challenges. The World Health Organization (WHO) reported that as many as 17 million people succumb each year to various infectious diseases [34]. Although in 2008, the WHO claimed that there had been a change in the main health problems of the world from infectious diseases towards non-communicable diseases, this stance has recently been changed. The current pandemic of severe acute respiratory syndrome coronavirus 2 (SARS-CoV-2 or COVID 19) has underlined the fact that infectious diseases have now returned to be one of the main problems in global heath [35]. These emerging viral outbreaks usually appear suddenly and kill many people before the outbreak can be controlled by, for instance, widespread vaccination. Moreover, human immunodeficiency virus (HIV) and tuberculosis remain two important infectious diseases with a high mortality rate. The recent SARS-CoV-2 outbreak spread rapidly around the world, and the WHO then classified it as a global pandemic outbreak. To date, more than 135 million people have been infected by SARS-CoV-2 and about 2.9 million have died [36].

Extensive efforts have been applied to develop a reliable sensor for rapid detection of COVID 19. For example, Jiao et al. [37] described a DNA nanoscaffold-based platform that could be used for the detection and monitoring of COVID 19. The developed sensor was based on the hybrid chain reaction (HCR), which could quantify the target RNA of the SARS-CoV-2 virus. The mechanism of the fluorescence-based system is shown in Fig. 1. The rolling circle amplification (RCA) approach was employed to synthesize the DNA scaffold (Fig. 1a) and then to prepare the self-quenching nucleotide probes H1 and H2. H1 has as hairpin structure with 5-carboxyfluorescein (FAM) dye and black hole quencher (BHQ1)

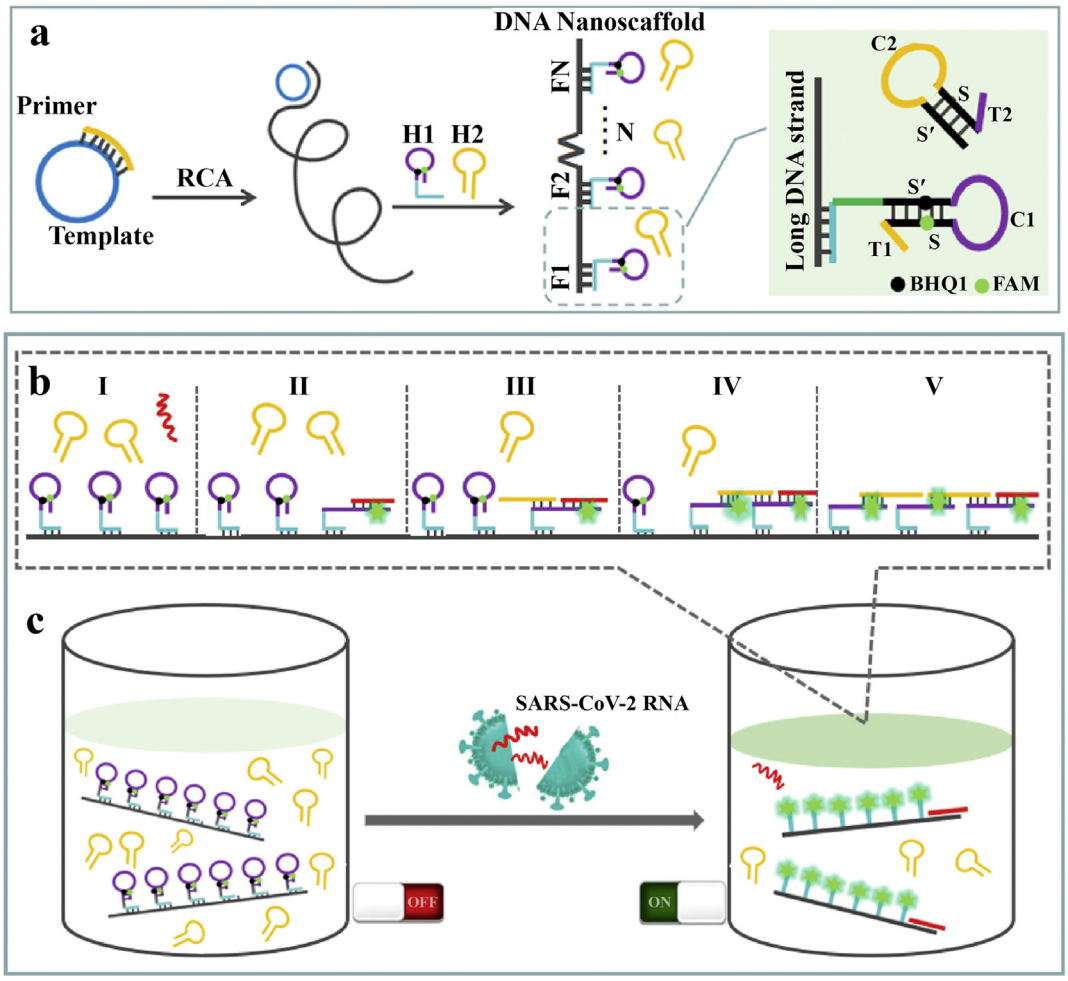

Fig. 1. Application of DNA scaffold for the detection of COVID 19. a) DNA scaffold synthesis, b and c) DNHCR based sensing of COVID 19. (FAM and BHQ1 are fluorescent dye and fluorescence quencher, respectively. Rolling circle replication (RCA) is a process in which DNA copies are produced. Tail T1 in H1 is complementary to C2 in H2, and tail T2 in H2 is complementary to C1 in H1. In the presence of RNA of SARS-CoV-2, it will hybridize with T1 and S, causing H1 to unfold to restore fluorescence (Scheme 1b II), and then H2 will hybridize with C1 and S′, causing H2 to unfold (Scheme 1b III) and continue to hybridize with adjacent H1 along the DNA nanoscaffold (Scheme 1b IV). Meanwhile, due to the compact arrangement of H1 on the DNA nanoscaffold, one target RNA can instantly light up the whole nanoscaffold with highly amplified signal gain (Scheme 1c).) (Copyright Science direct, 2020, reprinted with permission from Ref. [37], (License number: 4970230653752).

attached at either end as a dye-quencher pair. Tail T1 and T2 are complementary sequences to C2 and C1. In the presence of the RNA of SARS-CoV-2, firstly, RNA hybridizes with T1 and S, triggering H1 to open to restore the quenched fluorescence of FAM (Fig. 1b II), and then the H2 sequences hybridizes with C1 and S′, causing H2 to open (Fig. 1b III) and continue to hybridize with adjacent H1 along the DNA nanoscaffold (Fig. 1b IV). Because of the compact arrangement of H1 on the DNA nanoscaffold, a single target RNA can restore the fluorescence of the whole nanoscaffold with high efficiency (Fig. 1c). The 'turn-on' sensor was able to detect complementary RNA from 2 pM to 100 nM with a limit of detection (LOD) of 0.96 pM. The developed DNA-scaffold-based sensor shows the beneficial features of high fluorescence emission, rapid analysis time, high selectivity, and could be used an inexpensive sensing approach for COVID 19 detection. Although this probe could detect COVID19 DNA faster than the traditional quantitative real-time-polymerase chain reaction (qRT-PCR) assay, it is not suitable for population-wide screening because of its high cost and need for multiple steps in the sensor fabrication.

Besides viral infections, some infectious microorganisms such as bacteria are also dangerous pathogens that pose a major threat to human health. Setyawati et al. [38] conjugated gold nanoclusters (AuNCs) onto a DNA-scaffolded nanostructure to simultaneously detect *Escherichia coli* (*E. coli*) and *Staphylococcus aureus* (*S. aureus*) bacteria. The fabricated fluorescence-based platform provided a bright emission, and could be used as a reliable platform for the recognition of wide range of bacterial infections. Liu et al. [39] functionalized graphene scaffolds with a DNAzyme to develop another fluorescence-based sensor for *E. coli* detection. The DNAzyme was attached on the surface of graphene nanoparticles by non-covalent electrostatic bonds. Graphene efficiently quenched the fluorescence of a reporter dye attached to the DNAzyme, however, in the presence of *E. coli*, the fluorescent dye was released and its fluorescence was recovered. The 'turn-on' fluorescence was linear with *E. coli* concentrations from 10^5 to 10^7 CFU/mL. This probe could detect *E. coli* as low as 10^5 CFU/mL. Despite the low sensitivity of the system, the developed sensor was able to monitor in real-time, and could be made specific for other pathogenic bacteria.

The sensitivity of *E. coli* detection was further improved using barcode technology. Xu et al. [40] employed poly(ethyleneglycol) (PEG) hydrogel scaffolds to produce a barcode-based bacterial

detection approach. The porous nature of a hydrogel can increase the surface area available to interact with the bacteria. The developed aptamer-based system could simultaneously detect *S. aureus* and *E. coli* in spiked blood samples. The aptamer-based sensor showed higher sensitivity than the approach reported by Liu et al. [39] with a LOD of only 100 CFU/mL. The analysis time was about 2.5 h, which was shorter than commercial devices, which are currently used as a "gold standard" in the clinic, and they suggested the method could be a potential candidate for rapid detection of bacterial infections.

PEG-stabilized gold nanoparticle (AuNP)-based scaffolds were also used to quantify *S. aureus* bacteria. The results showed that PEGylated AuNPs could efficiently be conjugated to *S. aureus* specific phages by amide bonds. Although this approach could not provide quantitative data in biological samples, the system could be further improved for future application in biological media [41].

Label-free sensors have been investigated to provide real-time detection of biomolecules, without any need for sample pretreatment. Zhang et al. [42] reported that silver nanoclusters (AgNCs) modified with a DNA hairpin template could be used as a scaffold to monitor *Salmonella typhimurium (S. typhimurium)*. Upon binding of *S. typhimurium* to the scaffold material, the fluorescence intensity was increased. This system had the advantage of being able to differentiate living bacteria from dead or denatured ones, and displayed the specificity and ability to detect in real samples. Also, its label-free nature is an advantage, which provides a simple assessment technique.

Mobed et al. [43] reported an electrochemical biosensor for the determination of *Legionella pneumophila (L. pneumophila)*. They modified the surface of a gold electrode by electrodeposition of AuNPs/chitosan scaffolds, and then DNA sequences complementary to *L. pneumophila* cells were anchored. This sensor could measure ultra-low concentrations of DNA of *L. pneumophila* even at the zeptomolar level. In another study, amine-functionalized magnetic silica nanoparticles ($MNP@SiO_2@NH_2$) were used for the detection of *Yersinia enterocolitica*. $MNP@SiO_2@NH_2$ NPs were further functionalized with feroxamine to allow specific attachment to the bacteria by the interaction between feroxamine and the feroxamine receptor (FoxA). Despite the good selectivity of this system, the sensitivity was not satisfactory [44].

In conclusion, the development of sensitive and specific methods or devices for the detection of pathogenic microorganisms could be beneficial for world health. As the COVID 19 outbreak has shown, cheap and simple methods that still have high accuracy; could be rolled out worldwide, even to less developed countries. For bacteria detection, DNA hairpin-based sensors [42] showed the best performance, regarding simplicity and sensitivity of the developed sensor, however, the electrochemical DNA sensor reported by Mobed et al. [43] showed favorable analytical performance for bacteria detection.

2.2. Cancer diagnosis

Cancer has continued to be a major cause of human suffering and death around the world, despite a vast research effort. To control the cancer epidemic, one important strategy is to provide an early-stage diagnosis with wide coverage and more efficient results. Early diagnosis is mainly achieved by the detection and quantification of biomarkers related to cancer incidence and progression [45]. Biomarkers are biological molecules that can be detected in body fluids, and their levels often increase in the progress of the disease. Biomarkers play a key role in the screening of malignant tumors in the early phase of development. They are also important in the choice of treatment approach, assessing the treatment efficacy, mitigating treatment toxicity, and detecting any recurrence of the disease [46]. Although various types of biomarkers have been found in tumors and in cancer cells, most of the well-known cancer biomarkers that have been detected by biosensors have been protein-based [47,48]. Several conventional assay-based techniques, including polymerase chain reaction (PCR), flow cytometry, and immunohistochemistry have been exploited for the quantification of various biomarkers [49–53]. However, biosensors have recently attracted attention for the early diagnosis of cancer biomarkers because of their simplicity and rapidity [54]. A wide range of scaffold-based materials have been investigated as tools for the detection of cancer due to their advantages such as, high surface area, porosity, mechanical strength, and non-toxicity.

2.2.1. Protein biomarkers

Several cell-surface protein biomarkers such as, human epidermal growth factor receptor 2 (HER2), prostate-specific antigen (PSA), carcinoembryonic antigen (CEA), telomerase, protein tyrosine kinase-7 (PTK7), alkaline phosphatase (ALP) etc. have been used for the detection of cancer using various techniques [55–60].

PSA is an important biomarker for assessing the presence and progression of prostate cancer, and has been quantified using various analytical methods [61]. DNA scaffolds are useful biomaterials with superior properties such as low nonspecific adsorption, for the recognition of many biomolecules [62]. Chen et al. [63] developed an immunosensor using horseradish peroxidase (HRP) conjugated-AuNPs (gold nanoparticles) and a deoxyribonucleic acid (DNA) scaffold for the determination of PSA. The sensitivity of PSA detection depended on the distance between immobilized antibodies and the AuNPs, which acted as a signal reporter and amplification agent. Use of the DNA nanostructure-based scaffold allowed favorable binding of the antibodies to the PSA molecules resulting in high sensitivity with a detection limit (LOD) of 1.0 pg/mL. The DNA nanostructures provided a 3D substrate for the facile assembly of the biomolecules on the surface. Besides the sensitivity, the reported method suffered from a narrow dynamic range, which affected the reliability of the fabricated platform. In addition, it is not easy to construct this probe; and specialized conditions are needed for the storage of the sensor constituents. Also, DNA scaffolds were used to develop an electrochemiluminescence (ECL) sensor for the determination of telomerase activity. Telomerase is a eukaryotic ribonucleoprotein (RNP) complex which prevents cell death by maintaining the telomere length. Telomerase is over-expressed in cancer cells compared to normal cells, so it could be a key biomarker in cancer diagnosis [54]. DNA tetrahedral scaffolds acted as a connecting bridge between cadmium sulfide-quantum dots (CdS-QDs) and luminol labeled AuNPs (L-AuNPs). The CdS QDs were deposited onto glassy carbon electrodes (GCE) which were further modified with DNA tetrahedral scaffolds *via* thiol groups binding to AuNPs. In the presence of telomerase, the ECL signal was enhanced with a LOD of 2.03×10^{-9} IU for CdS QDs and 1.45×10^{-9} IU for luminol-based SPR-ECL sensors. The analytical performance was about two orders of magnitude better than conventional ELISA assays, furthermore, low false positive and false negative results were obtained using this sensor [64].

The cell membranes of both cancer and normal cells contain specific receptors, which are active in cell signaling pathways. These surface receptors have been used for diverse purposes in cancer including, sensing [65–68], drug delivery [69,70] and therapy [69,71]. The human epidermal growth factor receptor 2 (HER2) protein is a member of the epidermal growth factor receptor family. Over-expression of HER2 plays an important role in the development and progression of many epithelial malignancies, including breast, lung, prostate, bladder, ovarian, pancreas, and oral cancers.

Gu et al. [72] produced a nanocomposite containing carbon dots (CDs)@ZrHf-metal organic frameworks (MOF) by embedding a bimetallic ZrHf MOF into the amino-functionalized CDs for allowing immobilization of HER2-specific aptamers (Fig. 2). This method could simultaneously detect soluble HER2 as low as 19 fg/mL, and HER2-overexpressing MCF-7 cells over a range of 100 to 10^5 cells/mL. The exceptional properties could be attributed to the large specific area, high stability, and electrochemical activity of the scaffolds. However, aptamer-based approaches may suffer from the high cost of fabrication and limited storage of the fabricated sensors. Generally, metal-based scaffolds provide high conductivity, resulting in a highly sensitive platform. Despite the use of metals in the structure of the sensor, the scaffold was still biocompatible because the CDs totally covered the surface of the MOFs.

MOFs were also used to develop a scaffold-based biosensor to quantify carcinoembryonic antigen (CEA, a glycoprotein) [73]. CEA can be used in the clinical diagnosis of several types of cancer [74]. Guo et al. [73] produced a biosensor based on AgNCs@Apt@UiO-66. The scaffold-based sensor was fabricated using gold nanoclusters (AuNCs), zirconium metal–organic framework (Zr-MOF, UiO-66), and a CEA-targeted aptamer (Fig. 3). The AgNCs@Apt@UiO-66-based bifunctional biosensor showed high sensitivity for quantifying CEA with a linear range of 0.01–10 ng/mL using differential pulse voltammetry (DPV) or electrochemical impedance spectroscopy (EIS) techniques and 1.0–250 ng/mL for the surface plasmon resonance (SPR) technique. The AgNCs@Apt@UiO-66 nanocomposite showed good electrochemical activity, large specific surface area (due to UiO-66), and a high loading capacity, and displayed specific long-lasting binding to CEA. Despite various outstanding features of this sensor, its synthesis process and biocompatibility are questionable.

Bimetallic MOFs exhibit a synergistic effect and improved physicochemical properties compared to their monometallic counterparts. Zhou et al. [75] synthesized a bimetallic MOF-on-MOF nanocomposite for the detection of tyrosine-protein kinase-like 7 (PTK7, a cell membrane protein). They designed an aptasensor based on two bimetallic composites of Zn-MOF-on-Zr-MOF and Zr-MOF-on-Zn-MOF where the ZnZr-MOF acted as a scaffold substrate for immobilizing the aptamer *via* carboxyl and amine groups. Zr-MOF facilitates the immobilization of the PTK7 aptamer, and the Zn-MOF stabilizes the G-quadruplex formation. The Zn-MOF-on-Zr-MOF-based aptasensor showed high sensitivity compared to the Zr-MOF-on-Zn-MOF-based aptasensor for the detection of PTK7 with a dynamic range from 1.0 pg/mL to 1.0 ng/mL. They showed remarkable selectivity for PTK7 in the presence of interfering substances such as human serum, coupled with good stability, and reproducibility.

A near-infrared (NIR) fluorescent method was developed by Park et al. [76] for the detection of alkaline phosphatase (ALP, a cancer biomarker) [77]. Two enzyme-cleavable fluorescent probes (NIR-Phos-1 and NIR-Phos-2) were used for the modification of 3D-calcium deficient hydroxyapatite (CDHA) scaffolds, to fabricate a "turn-on" sensor. Upon cleavage of the phosphate groups of the probes by ALP, the produced fluorescence was linear up to 1.0 U/mL. Both NIR-Phos-1 and NIR-Phos-2 probes could detect ALP within 1.5 s, showing the potential for rapid and real-time detection. Because phosphate compounds can bind to bone with high affinity, the bone-like scaffold material could be effective for *in vivo* detection of ALP after implantation within the body for early-stage detection of bone metastasis. The use of a NIR-based probe has multiple benefits, including low-background emission, high signal-to-noise ratio, and non-invasive detection.

Exosomes are small (nanoscale) vesicles that are secreted from a variety of cells, and are released into the extracellular space where they can be detected in various body fluids. Exosomes play an important role in many physiological and pathological processes. They contain nucleic acids (DNAs and RNAs), lipids, and proteins that are characteristic of their source cell type. Exosomes can serve as biomarkers for the early diagnosis and prognosis of cancer. Chen et al. [78] developed an on-chip device using 3D-polydimethylsiloxane (PDMS) coated zinc oxide (ZnO) nanowires to enhance the sensitivity of exosome detection. A horseradish peroxidase (HRP)-labeled antibody was immobilized on the ZnO nanowire surface to detect the exosomes. The colorimetric biochip had high sensitivity, was easy-to-use and inexpensive, and could detect exosomes in cancer patients. There are various types of

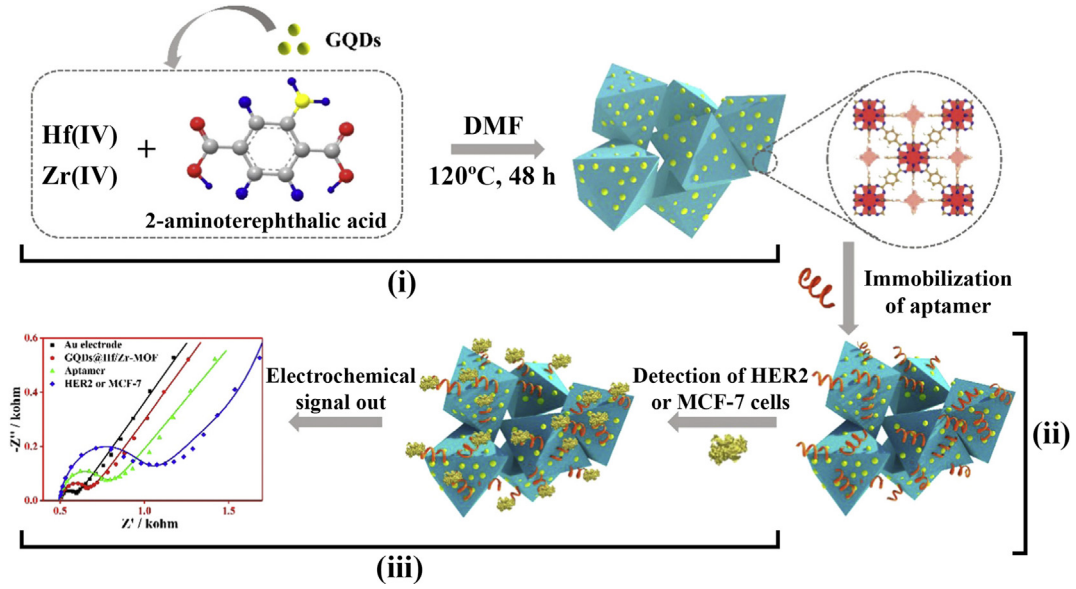

Fig. 2. Schematic diagram of CDs@ZrHf-MOF-based aptasensor for sensing HER2. (i) Synthesis of the nanocomposites; (ii) assembly of aptamers; (iii) detection of HER2 with EIS technique. (Copyright Science direct, 2020, reprinted with permission from Ref. [72], (License number: 4925840868034).

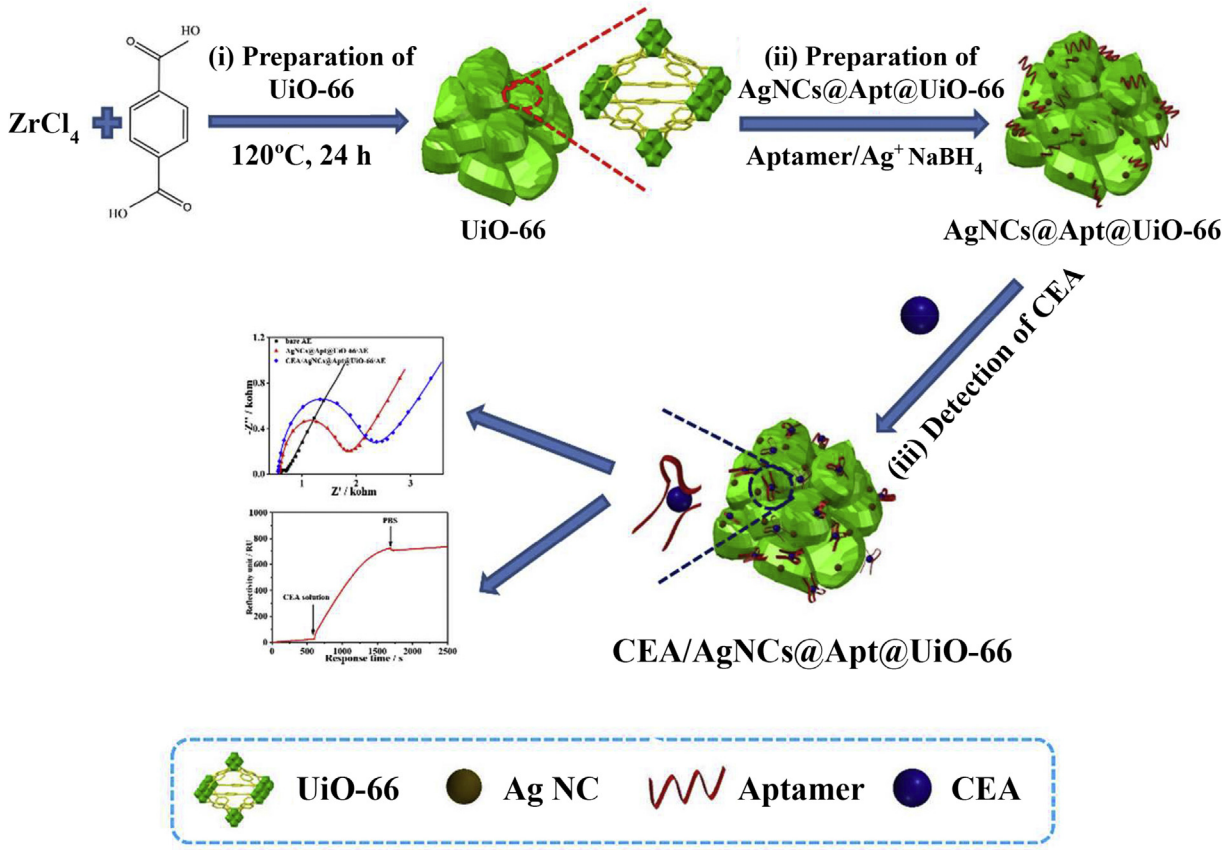

Fig. 3. AgNCs@Apt@UiO-66-based aptasensor for sensing CEA. (i) Synthesis of UiO-66; (ii) Synthesis of AgNCs@Apt@UiO-66; (iii) Measurement of CEA by electrochemical technique. (Reprinted (adapted) with permission from Ref. [73]. Copyright (2020) American Chemical Society).

surface proteins that could act as biomarkers of exosomes (such as CD63, CD171, CD81, CD9, EGFR and TSG101), so that several antibodies and aptamers could be used in scaffold materials to improve the sensitivity of detection of exosomes. Despite the novelty of the sensor, its sensitivity was not acceptable for detection in real samples.

Electrochemical and optical-based methods have mainly been used for the detection of protein-based biomarkers. These sensors have advantages of good bioanalytical performance, simplicity, possible miniaturization, low-cost and rapid fabrication procedures. The combination of scaffold materials with other advanced materials could enhance the sensitivity and specificity of biosensing approaches, and enable the detection of biomolecules in more complex environments. Despite the sensitivity of these biosensors, the biocompatibility and leachability of these complex nanomaterials in biological media needs further study before the devices can be submitted for regulatory approval. Some of the reports showed good potential for future development of point-of-care (POC) devices. For example, a NIR-based sensor reported for the detection of ALP provided various outstanding features, of high sensitivity, low noise and background emission, and simple fabrication steps [76]. In addition, an AgNCs@Apt@UiO-66-based bifunctional sensing system for CEA detection could be further applied for simultaneous detection of other analytes in a single POC device.

2.2.2. Nucleic acid-based biomarkers

MicroRNAs (miRNAs) are a group of endogenous non-coding small RNAs that are involved in a variety of biological processes. The abnormal expression of miRNAs in living cells and tissues (both up and down) can serve as a diagnostic marker for many cellular processes and diseases. A novel aptamer-incorporated Y-shaped backbone-rigidified triangular DNA scaffold (YTDS) was developed to detect and image miRNAs in living cells using fluorescence technique. The aptamer incorporated YTDS scaffold was functionalized with a DNAzyme walker construction, and could be taken up by the cancer cells without any need for transfection factors. This method was biocompatible with high sensitivity, and could be used for biological research and early diagnosis of diseases involving miRNAs [79]. The same strategy i.e. DNA walkers was utilized in an electrochemical DNA sensor by Wang and colleagues [80]. They fabricated a sensitive biosensor based on a DNA-tetrahedron (TDN) scaffold by attaching one of two enzymes either glucose oxidase (GOx) or HRP at the vertices. The edge length of the tetrahedron could be varied to control the inter-enzyme distance for maximum catalytic activity. Exonuclease III (Exo III) converted the target DNA to DNA2 (a DNAzyme) and upon hybridization between output DNAzyme and its substrate, the enzyme-modified segment was released from the TDN. After specific cellular internalization, endogenous miRNA initiated the progressive movement of the DNAzyme walker, during which a series of Na^{+}-dependent cleavage events occurred with the help of toehold-assisted hybridization. This biosensor showed high sensitivity, controllability, and biocompatibility with a low LOD of 3.0 fM DNA. In cancer patients, the amount of DNA released into the plasma is increased compared with healthy individuals. Therefore, DNA can be used as a biomarker for the diagnosis and monitoring of tumors in a non-invasive manner [54].

Electrochemical biosensors are suitable for miniaturization, due to the easily accessible portable signal-recoding instrument, possibility of a disposable stick for single use, and simple fabrication procedure. However, often enzyme-based sensors suffer from low-stability and high cost of the sensor fabrication.

2.2.3. Cytosensing of cancer cells

The early-stage detection of a very small number of cancer cells is one of the main unsolved problems in cancer diagnosis. Thus, approaches that could detect vary rare cancer cells that are present in biological fluids (blood or urine) are of importance in cancer detection. However, the approaches must be specific and sensitive, and able to differentiate cancer cells from normal cells in the presence of various interfering substances. A number of different strategies have been used to detect cancer cells, including aptamers, surface receptors, antibodies, etc. Soleymani et al. [81] summarized the reported approaches for the detection of cancer by recognition of the folate receptor (FA) which is often over-expressed on cancer cells. Moreover, other receptors (such as glycan, hyaluronic acid, etc.) not only have been used for cancer cell detection, but have also used for imaging [82], drug delivery [83] and theranostic applications [84].

Yu et al. [85] reported an aptamer-based platform for the detection of HL-60 cells. They used an aptamer-modified scaffold with magnetic beads and AuNPs to develop a colorimetric probe. The AuNPs could amplify the magnetic effect providing an ultra-sensitive colorimetric assay for cancer cells using the naked eye. This platform successfully identified HL-60 cancer cells in serum, and could be used as a point-of-care (POC) device for cancer detection. Generally, colorimetric approaches are less sensitive than other rapid detection techniques i.e. luminescence and electrochemical, however, the reported LOD for HL-60 cells was favorable which was mainly due to the aptamer. Aptamers can enhance the selectively and thus the sensitivity of analytical approaches by accurate recognition of analytes.

Biosensors are usually employed to detect circulating tumor cells, but in principle, these methods could also be used in solid tumors. To overcome this problem, superior tissue digestion approaches are needed to separate the cells from the extracellular matrix without any effect on the integrity of the cancer cells.

3. Determination of pharmaceuticals and drugs

The use of pharmaceutical drugs has become ubiquitous in modern medicine, but is not without its own risks. Possible overdose of drugs, and differences in pharmacokinetics between individual patients, can lead to serious risks to human health and can result in disorders of major internal organs, especially the liver [86,87]. Some drugs can enter the human body *via* food and water due to their very low biodegradability in the environment, and then cause serious health problems [88–90]. Furthermore, some drugs such as antibiotics decrease the resistance to new pathogens by killing beneficial bacteria within the body, and weaken the host immune system [91]. Therefore, accurate and sensitive monitoring of drug concentrations, without the interference of other analytes is of particular clinical importance.

Recently, Su et al. [24] exploited a 2D AuNCs@521-MOF nanocomposite coupled with a cocaine aptamer to modify the working electrode surface for the determination of cocaine. The optimized MOF scaffold-based aptasensor exhibited a wide dynamic range from 0.001 to 1.0 ng/mL with a low LOD of 0.44 and 0.75 pg/mL using the EIS and DPV techniques, respectively. The developed 2D AuNCs@521-MOF based platform showed good biocompatibility, large surface area, physicochemical stability, an active electrochemical performance and strong bio-affinity toward biomolecules bearing phosphate groups, which could be used for the recognition of other analytes in cell biology studies. Ultra-high sensitivity is the main benefit of the fabricated aptasensor, while the disadvantages are being time-consuming and expensive.

In another work, aptamers were used in a surface-enhanced Raman spectroscopy (SERS)-based approach for the recognition of cocaine using a combination of crystal violet-loaded mesoporous silica (MSN) scaffolds coupled with cocaine-specific aptamers [25]. Crystal violet acts as an efficient SERS reporter in the presence of gold nanotriangles (AuNT@PEG). SERS-based methods can be powerful analytical tools for the detection of pharmaceuticals because of their advantages, such as being label-free, sensitive and specific. The reported SERS-based system was able to detect low cocaine concentrations without any interference from biological substances or other drugs. This method was evaluated as a label-free method with high sensitivity (LOD, 10 nM), which can be further validated for use in forensic and therapeutic drug monitoring purposes.

Paracetamol (acetaminophen) is a widely used non-steroidal anti-inflammatory drug, which lowers the production of prostaglandins and reduces pain. Because it can also damage the liver, accurate determination of paracetamol concentrations is of great importance. Gowthaman and colleagues [26] reported an electrochemical scaffold-based platform for acetaminophen detection based on silver phosphate nanoparticles (AgP-NPs), which were used to modify a screen-printed carbon electrode (SPCE) (Fig. 4). The developed aptamer exhibited a linear range from 1.0 to 1000 μM and 0.1–1900 μM, a LOD of 17.6 nM and 0.39 nM with sensitivity of 1314.5 μA/μM/cm^{-2} and 2244.4 μA/μM/cm^{-2} for DPV and amperometric techniques, respectively.

Natural scaffold materials are an important class of materials benefiting from a sustainable and green chemistry approach. For example, superfolded green fluorescent protein (sfGFP) is a highly fluorescent protein derived from *Aequorea victoria*. Swift et al. [92] developed an aptasensor for the detection of chloramphenicol, which is an old antibiotic derived from *Streptomyces venezuelae* [93]. The scaffold structure of the sfGFP provided an effective contact between a chloramphenicol-specific DNA aptamer, enabling optical detection of chloramphenicol in biological samples. To enhance the sensitivity, ZnS:Mn NCs were added to the sfGFP-aptamer and then applied for colorimetric detection of chloramphenicol. The sfGFP-aptamer@ZnS:Mn NCs-based probe could determine chloramphenicol from 1.0 to 300 μM. Despite the high emission quantum yield of green

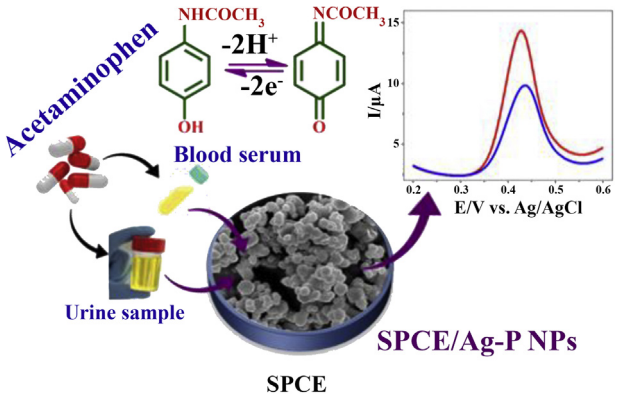

Fig. 4. Schematic illustration of the fabrication of SPCE using scaffold-based AgP-NP materials for the detection of acetaminophen concentrations in urine and blood using DPV technique. (Reprinted (adapted) with permission from Ref. [26]. Copyright (2020) American Chemical Society).

fluorescent proteins, the stability for fabrication of reliable sensors is questionable.

Heparin and protamine are both polyionic drugs, which are used as anticoagulants in clinical practice, but excessive concentrations can cause dangerous adverse effects [94,95]. Dey et al. [96] synthesized flower-like AuNP scaffolds for ultrasensitive detection of protamine and heparin in human serum samples. These scaffold materials were self-assembled on the surface of AuNPs and then attached to the surface of an electrochemical electrode using a thiol-functionalized 3D-silicate (3-(mercaptopropyl)trimethoxysilane (MPTS)) network. The developed electrochemical quartz crystal microbalance (QCM) showed high sensitivity for the detection of heparin and protamine at 0.05 μg/mL levels. Although, the authors determined heparin and protamine in laboratory plasma samples, the application in real samples remains to be confirmed.

A composite comprising multi-walled carbon nanotubes (MWCNTs), chitosan hydrogels (CHI), and hydroxyapatite nanoparticles (HANPs) was prepared in a simple ultrasonic method i.e. HANPs@MWCNT-CHI for the detection of nitrofurantoin (an antibacterial agent). The produced HANPs@MWCNT-CHI scaffold was used to modify the surface of GCE for accurate and sensitive detection (Fig. 5). The EIS, CV, and DPV techniques were utilized to record electrochemical signals. This sensor exhibited synergistic electrocatalytic activity between the components to detect nitrofurantoin with a sensitivity of 0.16 $\mu A \mu M^{-1} cm^{-2}$, resulting from the high surface-area-to-volume ratio of HANPs@MWCNT-CHI [91].

Bimetallic MOFs are a type of MOF that can have synergistic effects. Wang et al. [97] synthesized a series of bimetallic MOFs using CeO_2/CuO_x@mC nanomaterials (as scaffold) by calcination at high temperatures. The fabricated nanocomposites had a high specific surface area and were used as a substrate for the immobilization of an aptamer for the electrochemical detection of trace amounts of tobramycin (TOB, an antibiotic) in human serum and milk. This aptasensor was based on a CeO_2/CuO_x@mC900 nanocomposite and showed a wide linear range of TOB concentration from 0.01 pg/mL to 10 ng/L with a LOD of 2.0 fg/mL. The developed MOF-derived aptasensor could be applied in the biosensing of different antibiotics. The porous and bimetallic nature of the MOFs enhanced the detection sensitivity of TOB.

In conclusion, various analytical techniques have been applied to determine pharmaceuticals in biological media. Both spectroscopic techniques and electrochemical-based methods were have been employed. MOF nanostructures have been broadly used in sensing of pharmaceuticals, due to their high conductivity and abundant vacant orbitals to allow efficient readouts.

Regarding the analytical performance of the reported scaffold-based materials in drug sensing, the MOF-based method for detection of TOB [97] could be the best example of scaffold-based pharmaceutical sensors due to its high specificity, sensitivity, stability, and reliability.

4. Glucose monitoring

Glucose acts as a primary source of energy production in cellular metabolism, but the blood glucose concentration is elevated in diabetes [98]. The normal blood glucose concentration is on the range of 80–120 mg/dL (4.4–6.7 mM) [99]. The abnormal levels of glucose found in diabetes can cause kidney failure, high blood

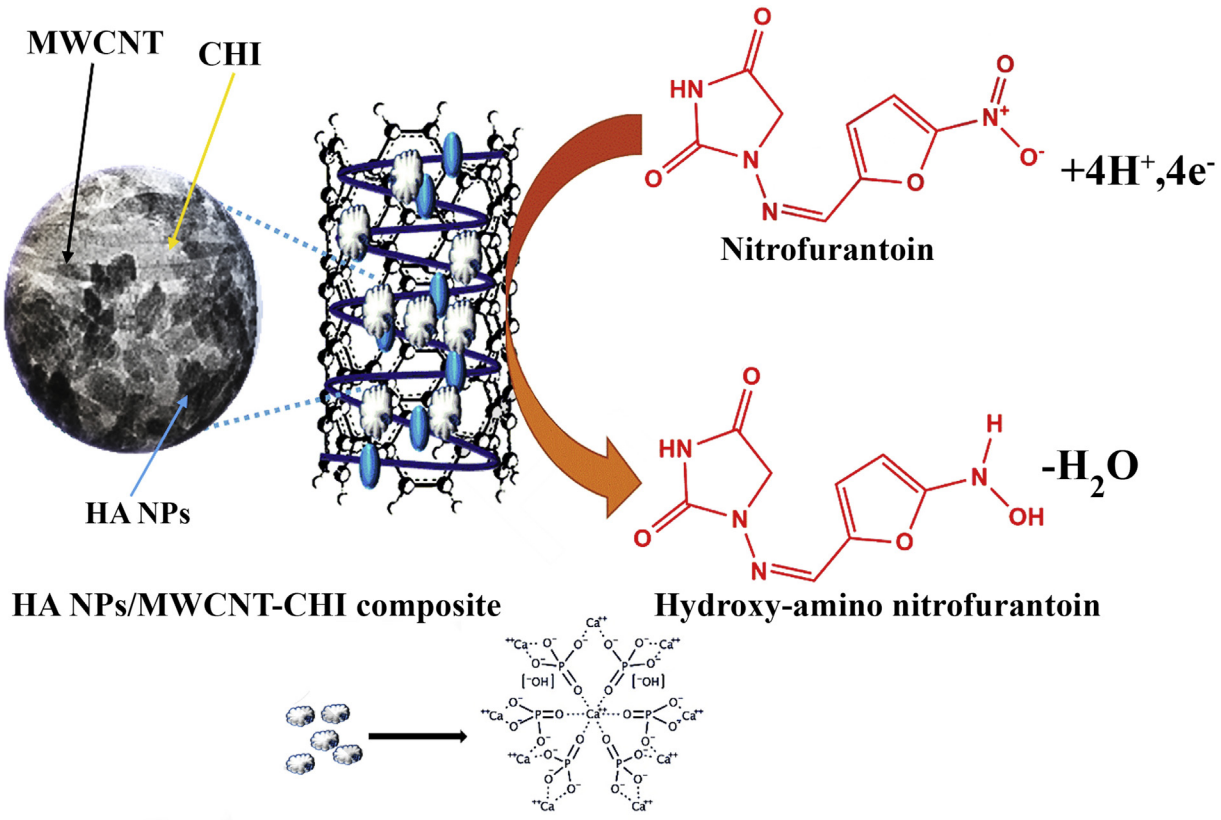

Fig. 5. Schematic illustration of the detection and electrochemical reduction of nitrofurantoin by HA NPs/MWCNT-CHI modified GCE. (Copyright Science direct, 2020, reprinted with permission from Ref. [91], (License number: 4925841098764).

pressure, stroke, heart disease, and blindness [100]. Therefore, rapid and accurate measurement of blood glucose levels are of great clinical importance [101]. The developed sensors can be categorized into enzyme-based and enzyme-free probes. Conventionally, enzyme-based probes can successfully determine the glucose level in human blood samples, but they usually suffer from the limited stability of the enzyme. Non-enzymatic spectroscopic and electrochemical sensing systems provides cheap and stable platforms, which can be used for POC testing and real-time detection of glucose concentrations in biological media.

To date, various materials have been used for detection of glucose based on electrochemical and optical techniques. In this subsection, the use of scaffold-based materials is discussed. Various types of scaffolds have been exploited in biosensors using different methods for glucose detection [102], that display high performance, rapid response time, high sensitivity, selectivity, and low cost [103].

4.1. Enzyme-free glucose sensors

Enzyme-free glucose sensors can directly determine glucose *via* electrocatalytic oxidation (electrochemical readout) and molecular recognition (optical readout), which do not involve expensive enzymes [104]. The outstanding features of enzyme-free glucose probes are their cheapness, reliability, low toxicity, and high catalytic effects.

Among the different optical sensing systems, fluorescence-based glucose determination probes have attracted much interest. For example, Balaconis and colleagues [21] developed an optical *in-situ* sensor based on a boronic acid scaffold. They used a competitive binding strategy between glucose molecules and a dye to bind to 4-carboxy-3-fluorophenyl boronic acid. The obtained results showed that the scaffold-based nanofiber was stable within the implantation site in tissue. Despite the novelty of the fabricated nanoprobe, its analytical performance was not evaluated, so more studies are needed to confirm its possible use for quantitative or semi quantitative detection of glucose. Due to the *in vivo* stability and high biocompatibility of the boronic acid-based nanofibers, these materials could be used for continuous monitoring of glucose concentrations within the body. However, other analytes could also be detected by this method with proper changes to the instrumentation and specific sensing agents. To enhance the biocompatibility of the implantable platforms for glucose sensing, Young et al. [23] used 3D porous collagen-based scaffolds for the sensor design. Moreover, the biocompatibility of the produced scaffold was further improved using nordihydroguaiaretic acid (NDGA) and glutaraldehyde (GA). The *in vivo* stability of the scaffold-based platform revealed that it decreased about 30–60% after one week of implantation, and thereafter remained unchanged. Despite the ability to measure biological concentrations of glucose (4.4–6.7 mM), this method sufferred from delayed action time, unfavorable analytical performance, and importantly low stability of the synthesized scaffold within the body [105]. Implantable sensors can continuously monitor analyte concentrations in the blood, however, the reliability of these types of glucose sensors is questionable, and additional experimental studies are needed to develop more reliable implantable sensors. Collagen-based scaffolds have also been utilized to fabricate a flexible electrochemical device for the determination of glucose. An electroconductive hydrogel (ECH) was used as a scaffold material for *in vivo* monitoring of glucose in plasma and tissue (porcine meat). This sensor was able to determine glucose levels up to 10 mM in about 100 s. The sensor could be designed as an injectable device for electrochemical monitoring of tissue glucose levels [106]. Despite its fast analysis time, the reported method cannot detect low concentrations of glucose, mainly because of the fact that some scaffold materials can block electron transfer from the electrolyte to the electrode surface during electrochemical detections. Table 1.

Over the last decades, carbon-based nanomaterials including CDs, GO, carbon nanotubes (MWCNT and SWCNT) fullerenes, etc. have been exploited as efficient scaffold materials for the detection of glucose. Qian et al. [101] utilized a fiber microelectrode based on thin nickel hydroxide $Ni(OH)_2$ nanosheets incorporated into CNTs as a highly-aligned scaffold. The fabricated sensor displayed an excellent analytical performance, with a wide dynamic range from 20 μM to 10.5 mM of glucose concentration and a LOD of 0.645 μM and a sensitivity of 12.2 $mAcm^{-2}mM^{-1}$. The modified fiber microelectrode showed high electrochemical activity, relatively high sensitivity (as compared with the above reported methods), and low-interference by coexisting agents, thus it could be used for the development of non-enzymatic glucose sensors in clinical applications.

Carbon-nanosheets-based scaffolds have the benefits of high electrical conductivity, large surface area, good stability, and could be useful for glucose determination. For example, graphene nanosheets were utilized to develop a scaffold-based glucose biosensor. Zhao and colleagues [103] used a 3D monolithic nanoporous gold (NPG) scaffold deposited onto graphene paper (GP) and then decorated with an ultra-fine layer of binary PtCo alloy nanoparticles for the detection of glucose. The developed PtCo/NPG/GP-based sensor was linear from 35 μM to 30 mM glucose with a low LOD of 5.0 μM, and sensitivity of 7.84 μA $cm^{-2}mM^{-1}$. The flexible electrochemical biosensor could be used as an implantable, mobile, and wearable device for the monitoring of glucose concentrations in patients.

GO sheets display high conductivity due to the high ratio of oxygen/carbon atoms, thus GO can be employed in the modification of electrochemical electrodes. Gowthaman et al. [22] developed a non-enzymatic electrochemical glucose sensor by the reduction of nitrogen-doped graphene oxide (N-GO scaffold) to produce nitrogen-doped graphene (NG). Then copper nanostructures (CuNSs) were electrodeposited onto the NG modified electrode to detect glucose in urine and serum samples (Fig. 6). The designed electrochemical sensor (GCE/NG-CuNS) showed a wide dynamic range from 50 nM to 5.0 mM of glucose with LOD of 14 nM and a sensitivity of 1848 $\mu AmM^{-1}cm^{-2}$. The electroactivity of the electrode modified by NG-dendritic CuNSs towards glucose was higher than other shapes of the CuNS nanoparticles. The excellent electrochemical performance of the NG-CuNS probe was attributed to the enhanced surface area of the GCE by NG-CuNS.

4.2. Enzymatic glucose sensors

Enzymatic glucose sensors have benefits like simplicity, high sensitivity, efficiency, and specificity, but they showed two major limitations of high cost and instability, caused by the use of enzymes [107].

Soylemez and co-workers [98] used poly(4-vinylpyridine) (P4VP) and SWCNT as a carbon-based scaffold, attached to a 3-bromopropyltrichlorosilane-treated gold electrode for developing a glucose sensor. The surface of the P4VP-SWCNT composite was functionalized by immobilization of GOx for the specific detection of glucose. The synthesized P4VP-SWCNT-GOx showed high selectivity, sensitivity and stability, and was able to recognize glucose within a relativity wide dynamic range. It must be noted that the P4VP-SWCNT-GOx device needs a dilution step to determine glucose in real biological fluids due to the relatively high blood level of glucose.

Incorporation of highly fluorescent colloidal nanomaterials into a biocompatible scaffold could provide an implantable sensor for personalized medical devices [108]. Xie et al. [109] encapsulated AuNRs and CdSe/ZnS quantum dots (QDs) into polyethylene glycol

Table 1
Summary of scaffold materials for biomedical sensing.

Material	Scaffold type	Technique	Analyte	Dynamic range	LOD(LOQ)	Ref.
Cancer biomarkers' detection (protein biomarkers)						
HRP-AuNPs/DNA	DNA	electrochemical	PSA	–	1 pg/mL	[63]
CdS QDs-GCE/DNA tetrahedral/L-Au NPs	DNA	SPR-ECL	Telomerase	–	2.03×10^{-9} IU (CdS QDs) 1.45×10^{-9} IU (luminol)	[64]
CDs/ZrHf-MOF	Metal-based	electrochemical	HER2	0.001–10 ng/mL (HER2) 100–10^5 cells/mL (MCF-7 cells)	19 fg/mL (HER2) 23 cells/mL (MCF-7 cells)	[72]
AgNCs/Apt/UiO-66	Metal-based	DPV EIS SPR	CEA	0.01–10 ng/mL 0.01–10 ng/mL 1.0–250 ng/mL	4.93 pg/mL 8.88 pg/mL 0.3 ng/mL	[73]
Zn-MOF-on-ZrMOF	Metal-based	EIS DPV	PTK7	–	0.84 pg/mL 0.66 pg/mL	[75]
NIR-3D- CDHA	CDHA	fluorescence	ALP	–	10^{-5}–10^{-3} U/mL	[76]
ZnO-coated 3D PDMS	Aptamer tetrahedral	colorimetric	Exosomes	$2.2 \times 10^5 - 2.4 \times 10^7$ particles/μL	–	[78]
Cancer biomarker detection (nucleic acid based biomarkers)						
Ap-YTDS/DzW	YTDS	Fluorescence	miRNAs	–	–	[79]
TDN scaffold/HRP/GOx	TDN	Electrochemical	DNA	0.01 pM–10 nM	3 fM	[80]
Detection of cancer cells						
Au NPs	Aptamer	Colorimetric	HL-60	10–10^4 cells/mL	10 cells/mL	[85]
Pharmaceutical detection						
2D AuNCs/521-MOF/cocaine aptamer	MOF scaffold	Electrochemical (EIS and DPV)	Cocaine	0.001–1.0 ng mL^{-1}	1.29 pM 2.22 pM	[24]
CV-loaded MSNS/cocain aptamer/AuNT/PEG	Mesoporous silica	SERS	Cocaine	–	10 nM	[25]
SPCE/Ag–P NPs	AgP-NPs	Electrochemical	Paracetamol	1–1000 μM 0.1–1900 μM	17.6 nM 0.39 nM	[26]
sfGFP/Car9-CT43 /ZnS:Mn nanocrystals	sfGFP	Optical	Chloramphenicol	–	–	[92]
AuNPs/thiol-functionalized 3D-silicate network	Flowerlike AuNPs	Electrochemical	Heparin	–	0.8 nM	[96]
HANPs/MWCNT-CHI/GCE	HA NPs/MWCNT-CHI	Electrochemical	Nitrofurantoin	0.005–982.1 μM	1.3 nM	[91]
CeO_2/CuOx@mC900/aptasensor	Bimetallic MOF	Electrochemical	Tobramycine	21 fM –21 nM	4.2 fM	[97]
AuNRs -loaded PEG capsules/Ca^{2+}-alginate hydrogel scaffold	Alginate hydrogel scaffold	Optical	Heparin	–	–	[109]
Glucose detection						
Nanofiber/derivatives of 4-carboxy-3-fluorophenyl boronic acid	Boronic acid	Fluorescence	Glucose	–	–	[21]
GCE/NG-CuNS	N-GO	Electrochemical l	Glucose	0.0005–5.0 mM	14 nM	[22]
GA- and NDGA-crosslinked porous collagen scaffolds	Collagen	Amperometric	Glucose	2–30 mM	–	[23]
ECH	Collagen	ChA	Glucose	up to 10 mM	–	[106]
GOx/MoS_2–TiO_2/ITO	MoS_2 nanosheets; TiO_2 nanorods	PEC	Glucose	0.1–10.5 mM	15 μM	[111]
$Ni(OH)_2$/CNT fiber	CNT	Electrochemical	Glucose	20 μM–10.5 mM	0.645 μM	[101]
P4VP-SWCNT/GOx film	SWCNT	Raman	Glucose	0.08–2.2 mM	–	[98]
PtCo/NPG/GP	3D-Nanoporous gold	Electrochemical	Glucose	35 μM – 30 mM	5 μM	[103]
Ag/α-Fe_2O_3/GOx/Nafion electrode	Spruce branched a-Fe_2O_3 nanostructures	Amperometric	Glucose	0.003–33 mM	1 μM	[102]
QD and AuNRs -loaded PEG capsules/Ca^{2+}-alginate hydrogel scaffold	Alginate hydrogel scaffold	Optical	Glucose	–	–	[109]
GCE/graphene/pectin-CuNPs	Pectin	Electrochemical	Glucose	10 μM–5.5 mM	2.1 μM	[133]
Neurotransmitter detection						
BSA–Pt NPs	BSA	Optical	Choline Acetylcholine	6–400 μM 10–200 μM	2.5 μM 2.84 μM	[28]
NeuroSensor 521 (NS521)/ coumarin-3-aldehyde scaffold	Coumarin-3-aldehyde	Fluorescence	Dopamine Norepinephrine Glutamate	–	–	[29]
PA-DS/CNTs/modified graphite electrode	PA-DS	Electrochemical l	Dopamine	–	–	[30]
Metal ions detection						
QG-scaffolded COFs	QG-scaffold	Fluorescence	Copper	0.0010–10.0 μM (blood) 0.0032–32.0 μM (waste water)	0.50 nM (blood) 2.4 nM (waste water)	[33]
ZnIC	Iminocoumarin	Fluorescence	Zinc	–	–	[121]
QD-Biopolymer TSPP	QDs-TSPP	Fluorescence	Zinc	0.05–4 μM	1 nM	[119]
Pyridine–pyridine	Pyridine–pyridine	Fluorescence	Zinc	0.25–100 μM	–	[120]
POEGMA-AuNP	POEGMA-AuNP	Colorimetry	Lead	0.1–100 nM	25 pM	[127]

(*continued on next page*)

Table 1 (*continued*)

Material	Scaffold type	Technique	Analyte	Dynamic range	LOD(LOQ)	Ref.
3D gyroidal mesoporous aluminosilica pellets	3D-Gyroidal mesoporous aluminosilica pellets	Optical	Mercury	–	1.4 nM	[117]
Hydrogen peroxide detection						
Thiolated HRP/AuNPs-PTA-TiO_2 nanotube	Tubular TiO_2 nanocluster	Electrochemical	Hydrogen peroxide	65–1600 μM	5 μM	[130]
Nanogel-coated biosensor	Nanogel	Electrochemical	Hydrogen peroxide	0.1–1.5 mM	2.5 μM	[131]
HRP/ZrO_2-grafted collagen/DMSO/GE	Collagen	Electrochemical	Hydrogen peroxide	1.0–73.0 μM	down to 0.25 μM	[132]
GCE/graphene/pectin-CuNPs	Pectin	Electrochemical	Hydrogen peroxide	1 μM–1mM	0.35 μM	[133]
AuNFs/IL–GF/paper electrode	IL/GF	Electrochemical	Hydrogen peroxide	0.5 μM–2.3 mM	100 nM	[134]
GC/Pd@MSM-SO_3H	MSM-SO_3H	Electrochemical	Hydrogen peroxide	47.0 nM–1.0 mM	–	[27]
Amino acid and enzyme detection						
BTP-Cys	BTP	Fluorescence	Cys	–	0.38 μM	[31]
AuNC–CoO	AuNCs and CoO	Electrochemical	Cys	0.1 nM–1.0 μM	16 pM	[32]
CNC/PVA/HEA-TDI (F-Acryl)	CNC/PVA	Fluorescence	Trypsin	–	–	[140]

3D-calcium deficient hydroxyapatite (CDHA), Y-shaped backbone-rigidified triangular DNA scaffolds (YTDS), tetrahedron (TDN) scaffolds, superfolded green fluorescent protein (sfGFP), Multi-walled carbon nanotubes/composite of chitosan hydrogel/hydroxyapatite nanoparticles (HA NPs/MWCNT-CHI) scaffolds, nitrogen-doped graphene oxide (N-GO), poly-(allylamine)/dodecyl sulfate (PA-DS), meso-tetra(4-sulfonatophenyl)porphine dihydro-chloride (TSPP), quantum dots (QDs), poly (oligo(ethylene glycol) methacrylate) (POEGMA) polymer functionalized AuNPs, ionic liquid (IL)/graphene framework (GF), 2,5-bis (benzo[d]thiazol-2-yl) (BTP), porous cellulose nanocrystal (CNC)/poly (vinyl alcohol) (PVA).

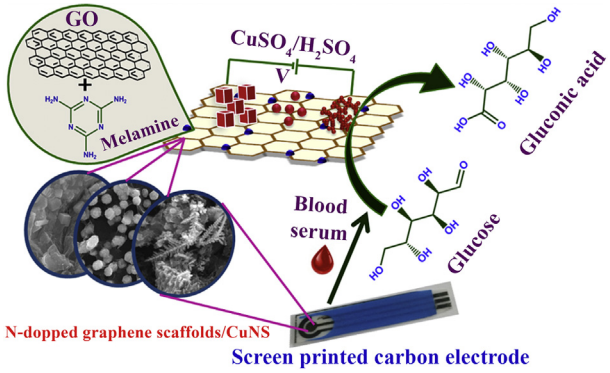

Fig. 6. Schematic illustration of a non-enzymatic electrochemical glucose sensor. The NG scaffolds were attached on the GCE surface and then modified by CuNSs. (Reprinted (adapted) with permission from Ref. [22]. Copyright (2020) American Chemical Society).

(PEG) microcapsules which were immobilized on the surface of calcium-alginate hydrogel scaffolds for the detection of small biomolecules. In the presence of glucose (or heparin), the QDs and AuNR-functionalized GOx probe showed optical signals depending on the glucose concentrations. These nanoconstructs could encapsulate different colloidal nanosensors, and be retained in the body as an implantable device for analyte sensing. The developed implantable biosensor could cover the biological concentration range of glucose. Despite its low sensitivity, this sensor could detect glucose over a wide range which covers the minimum blood level of glucose (3.9 mM). Photoelectrochemistry (PEC) is another type of electrochemical detection method, which relies on a electrochemical reaction between electroactive and photoexcited species that occurs at the interface between the electrolyte and the modified electrode [110]. Recently, Liu and co-workers [111] reported a PEC glucose biosensor based on a molybdenum disulfide (MoS_2)–TiO_2-NRs heterostructure to modify an indium tin oxide (ITO) electrode. GOx was assembled onto the surface of the MoS_2 nanosheet-TiO_2-NRs composite. The designed PEC-based biosensor showed a LOD of 15 μM of glucose with sensitivity of 0.81 μA $mM^{-1}cm^{-2}$ and a dynamic range of 0.1–10.5 mM. The produced nanocomposite showed the advantages of large surface area, good conductivity, and low energy band gap.

Ferric oxide has attracted attention due to its electrocatalytic properties. For example, Umar et al. [102] designed an amperometric glucose biosensor by modifying a silver electrode surface using spruce-like α-Fe_2O_3 nanostructures. The sensitivity of this biosensor was 85.384 $mAmM^{-1}cm^{-2}$, allowing sensitive detection of glucose within 2 s. Despite its favorable sensitivity, the application of this sensor in real samples was not reported.

In conclusion, implantable glucose sensors can act as POC devices for personalized medicine and for continuous *in vivo* detection of glucose. These types of biosensors are usually constructed from biocompatible materials with good *in vivo* stability. Implantable sensors can detect diseases at their earliest stages and can be applied for real-time detection of analytes. However, there are some questions that need to be addressed before the use of implantable sensors within the human body, including biocompatibility, stability, possible leaching in biological media, and long-term toxicity.

To introduce a well-defined sensor for glucose detection, some criteria must be considered, such as sensitivity (to support all biological concentrations of glucose), reliability, biocompatibility, and physical stability to be durable against leaching in biological media. A non-enzymatic sensor reported by Gowthaman et al. [22] was one of the best scaffold-based approaches for the detection of glucose due to its high sensitivity, biocompatibility, and possibility to be a portable POC device for *in situ* analysis.

5. Neurotransmitter biosensing

Neurotransmitters transfer information between nerve cells, muscles, organs, or other tissues [112]. Neurotransmitters can be different chemical compounds such as, amino acids, peptides, gaseous neurotransmitters, or biogenic amines [113]. Deregulation of neurotransmitters can be found in many diseases such as Parkinson's, schizophrenia, and Alzheimer's diseases. Therefore, monitoring the expression levels of neurotransmitters is of great clinical significance for early stage diagnosis and monitoring of treatment of neurological diseases [114]. Some notable scaffold-based approaches have been reported for neurotransmitter detection. For example, a bovine serum albumin (BSA) scaffold containing platinum nanoparticles (Pt NPs) was utilized by He and colleagues [28] for the detection of choline in infant formula and acetylcholine in plasma. Acetylcholine and choline react with acetylcholinesterase (AChE) and choline oxidase (ChOx) to produce H_2O_2, which was determined by an electrochemical method. The

developed BSA–Pt NP-based sensor exhibited excellent sensitivity and selectivity with a linear range from 6.0 to 400 μM and 10–200 μM, LODs of 2.5 μM and 2.84 μM for choline and acetylcholine, respectively.

Coumarin scaffolds are constructed from naturally occurring materials with high biocompatibility and the potential to be used in implantable sensors. Hettie et al. [29] developed a fluorescent platform called "NeuroSensor 521" (NS521). This platform consisted of a coumarin-3-aldehyde scaffold for the detection of primary-amine neurotransmitters of live chromaffin cells. Various types of coumarin-3-aldehyde scaffolds have been fabricated to develop a fluorescence-based sensor. This type of biosensor is based on the acceptor-excitation photo-induced electron transfer (a-PET) mechanism that could simultaneously detect glutamate, norepinephrine, and dopamine. In addition, the fabricated scaffolds were used for biological imaging and selective labeling of norepinephrine in living cells. It is noteworthy that glutamate, norepinephrine, dopamine, and serotonin are present in secretory vesicles at relatively high concentrations (300 mM − 1 M), so, this sensor could be utilized as a specific probe for detection in live chromaffin cells. Contrary to some other methods for detection of neurotransmitters, this sensor did not show good analytical features and the incorporated molecules may be toxic towards living cells.

Polyelectrolyte-surfactant polymers possessing charged polymeric chains and charged surfaces can form a stable film with CNTs coated on the surface of a graphite electrode to produce a scaffold substrate. Cortez et al. [30] used poly-(allylamine)/dodecyl sulfate (PA-DS) to improve the surface of a graphite screen-printed electrode to construct a sensing platform for dopamine. The polyelectrolyte-surfactant complex was used as a scaffold to support the CNTs. PA-DS-CNT modified electrode could catalyze the oxidation of dopamine, in the presence of an excess of ascorbic acid (100 folds).

Scaffold materials can improve the recognition of neurotransmitters by enhancing the surface of the nanoprobes, and increase the density of the immobilization sites on their surface. The 3D structure of scaffold materials not only affords high sensitivity but also enhances the stability of the sensors. Coumarin-based scaffolds could be used in the construction of implantable sensors for neurotransmitters.

6. Determination of inorganic ions

Increasing concerns about threats to human health and the need for ever more strict environmental protection has prompted active research on the toxicity of contaminating metal ions [115]. The presence of particular metal ions such as zinc and copper in the human body is essential for the normal functioning of cells, but abnormal changes in their concentration are closely related to the development of diseases such as Alzheimer's, cerebral ischemia, epilepsy, and diabetes [116]. In addition, metal ions such as cadmium, lead, mercury or copper in drinking water can cause various diseases, such as cancer, rheumatoid arthritis, kidney disease, nervous disorders and circulatory disorders, and are considered to be a major problem because of their high toxicity and destructive effects on both human health and the environment [117]. For these reasons, accurate and rapid quantification of ultra-trace levels of metal ions in environmental and biological samples can be considered as part of the effort to reduce the risk of a wide range of diseases [118].

Due to the intrinsic sensitivity of the fluorescence technique, a combination of fluorescent probes with 3D scaffold materials can enhance the sensitivity of the sensing approaches. For instance, Cai and colleagues [33] used a Q graphene (QG) scaffold-based metal-free fluorescent covalent organic framework (COF) for developing a novel biosensor for copper detection. The high density of functional groups on the edges of the hollow QG improved the surface properties and provided a strong attachment site for copper ions, resulting in fluorescence quenching of the probe. In addition, the QG-scaffold COF-based sorbents were able to remove copper ions from urban wastewater. The 3D structure of COFs provides highly specific detection along with an antifouling effect to remove possible interfering molecules from the surface of the fabricated probe. Because of the antifouling effect, an LOD of 50 pM was obtained using the COF-based probe.

Most recently, Liu et al. [119] used DNA functionalized QDs for the detection of zinc. In the structure of the fabricated platform, biopolymers decreased the interfacial thickness to about 2 nm, increasing the efficiency of the FRET mechanism about 60-fold. The sensor displayed a continuous color shift from yellow to bright green in the presence of zinc that could be seen with the naked eye. As a result, the new QD-FRET sensor had a reversible, high-resolution fluorescent imaging capability, and was low-cost and reliable for the detection of zinc. The produced scaffold provided a sensitive colorimetric sensor, which could be used for reliable *in-situ* sensing of zinc in living cells.

Pyridine–pyridone water-soluble scaffolds were applied for the fluorescent determination of zinc in living cells [120]. To increase the sensitivity of the pyridine–pyridine-based scaffolds, a fluorescence on/off sensor (4-[4-(methylsulfanyl)-2-oxo-6-(pyridin-2-yl)-1,2-dihydropyridin-3-yl]benzoic acid) was synthesized. The linear dynamic range of the probe was from 0.25 to 100 μM, and the scaffolds could be used for efficient bioimaging of zinc in cancer cells.

Komatsu and co-workers [121] developed a novel zinc fluorescence probe based on the iminocoumarin (IC) fluorophore as a scaffold and (ethylamino)dipicolylamine as a zinc specific chelator for the ratiometric imaging of intracellular zinc concentrations in living cells. In the presence of zinc, the fluorescence emission of the ZnIC probe shifted to the red wavelengths, and the probe showed high affinity and selectivity for zinc ions compared to other ions. This sensing probe had a high QY, long excitation wavelength, and was useful for investigating the biological functions of zinc.

The simultaneous detection of two or more different analytes not only decreases the time required, but also lowers the cost, and is suitable for screening purposes. El-Safty et al. [117] synthesized a 3D scaffold of gyroidal mesoporous aluminosilica pellets for ultra-sensitive simultaneous detection of copper, mercury, and cadmium ions. The reflectance-based sensor was able to detect these metal ions down to about 10^{-10} M. The high sensitivity of the sensor was due to the mesoporous nature of the material, with a large surface area-to-volume ratio. The long-term stability, reproducibility, and the reusability of the pellets were additional benefits, for ultra-fast detection and removal of multiple analytes ($\leq$1 min).

Colorimetric detection techniques are usually relatively simple to operate, and can provide the concentration of analytes without any need for instrumentation. Colorimetry is widely utilized for biomedical analysis and fabrication of several types of biosensors. Compared with other analytical techniques, the colorimetric platforms have some outstanding features including cheap and simple fabrication and easy detection, where in some cases the concentration of analytes can be determined without needing any instruments (naked eye). However, colorimetry-based platforms are generally low sensitivity approaches [122–126]. Ferhan and coworkers [127] fabricated a solid-phase colorimetric sensor for the detection of lead ions depending on an interaction with poly(oligoethylene glycol)methacrylate) (POEGMA) polymer functionalized AuNPs as a non-rigid scaffold. Solid phase cartridges provided a simple method to extract and determine the analytes by observing a color change to detect lead ions.

In conclusion, two types of scaffolds have been used for the detection of ions i.e. nanocomposites and organic based scaffolds. It appears that modified nanomaterials provide a more sensitive approach for metal ion detection. Technically, two methods (i.e. fluorescence and colorimetry) have been used to determine ions with scaffold-based materials; however, colorimetric methods have the potential to be used in portable devices for *in-situ* analysis.

7. Hydrogen peroxide monitoring

Hydrogen peroxide (H_2O_2) occurs in living organisms because it is naturally produced by cellular activities, but it can be damaging when present in an excessive concentration [128]. Regarding the lifetime and stability of hydrogen peroxide, it easily penetrates into the cells, and chronic exposure can cause changes in cellular functions including, DNA damage, cell apoptosis, protein synthesis, intracellular thermogenesis that could all lead to various diseases [129]. Therefore, considerable efforts have been devoted to the development of various methods for accurate and fast monitoring of H_2O_2 inside living cells [128].

Scaffold-based materials have also been used in combination with other nanomaterials for the detection of hydrogen peroxide. In 2013, an electrochemical enzyme-based sensor was fabricated for the detection of hydrogen peroxide based on a scaffold containing gold-titanium dioxide (TiO_2) nanotubes. In this probe, a hydrophilic ionic liquid, i.e. 1-decyl-3-methylimidazolium bromide and Nafion were applied to modify the surface of a GCE, and then thiolated-HRP was attached to the GCE surface as a model enzyme. The ease of electron transfer and the stability of HRP were increased by the strong affinity between AuNPs and the sulfhydryl group of the thiolated enzyme. The AuNPs were uniformly distributed onto the TiO_2 nanotubes, and the high specific surface area of both the AuNPs and the TiO_2 nanotubes increased the number of enzyme molecules that could be loaded and decreased their aggregation. This biosensor exhibited a LOD of 5 μM with a dynamic range of 65–1600 μM, and a sensitivity of 18.1×10^{-3} $\mu A \mu M^{-1}$. Due to the excellent biocompatibility, good conductivity, and low response time, this nanocomposite-based scaffold could be used as an efficient sensing element for enzymatic biosensors after enhancing the sensitivity of the probe [130].

To enhance the loading capacity of enzymes onto the scaffold, a flow-induced gelation method was used to immobilize enzymes on a nanoporous scaffold. The resulting nanogel was functionalized with HRP enzyme. Due to the structure of the scaffold nanogel, the nanogel-HRP showed high stability. The nanogel-based biosensor showed a linear amperometric response over the 0.1–1.5 mM range, with a LOD of 2.5 μM [131]. Also, Zong et al. [132] utilized zirconia nanoparticles to modify collagen scaffolds for hydrogen peroxide determination using HRP. The modified graphite electrode had advantages such as biocompatibility, and a high protein loading capacity, which allowed the sensor to detect hydrogen peroxide down to 0.25 μM. The high affinity of the materials for the enzyme provided the sensor with good analytical performance. Although enzyme-based sensors are highly selective toward their substrate analytes, their tendency towards instability, high cost, and slow analysis time all limit their real world applications. Furthermore, the sensing performance of the reported method do not necessarily cover biological hydrogen peroxide levels.

Recently, non-enzyme-based sensors have also attracted attention. In 2015, a non-enzymatic electrochemical sensor based on a scaffold of graphene/CuNPs and pectin modifying a GCE was reported for the determination of hydrogen peroxide. The developed amperometric sensor allowed successful determination of hydrogen peroxide (1 μM to 1 mM range) in plasma samples without any interference from coexisting substances. The electrocatalytic activity of CuNPs enhanced the sensitivity of the sensor up to 0 0.391 $\mu A \mu M^{-1}$ with a LOD of 0.35 μM [133].

Improved sensitivity was provided by using a porous gold nanoflower (AuNFs) and ionic liquid/graphene framework (GF) scaffold within a paper-based electrode. The developed non-enzymatic electrochemical sensor measured the hydrogen peroxide that was secreted from breast cancer cells. The signal was linearly proportional to the hydrogen peroxide concentration over a 0.5 μM - 2.3 mM range with a LOD of 100 nM. The sensitivity of the approach was 425.6 $\mu A cm^{-2} mM^{-1}$ [134]. The sensitivity was further increased using mesoporous silica microspheres (MSM) because of their large surface area, which provided abundant functional groups for interaction with analytes. In 2018, Gupta et al. [27] designed a sensitive enzyme-free electrochemical sensor based on a Pd@SO_3H-MSM nanocomposite to determine hydrogen peroxide in a wide linear range of 47.0 nM - 1.0 mM. The Pd@SO_3H-MSM was synthesized through electrostatic interactions between palladium ions and the $-SO_3H$ groups on to the surface of the MSM. Pd@SO_3H-MSM was used for fabrication of the scaffold on the GCE *via* drop-casting (Fig. 7).

Overall, two types of biosensors have been reported for hydrogen peroxide detection, i.e. enzymatic and non-enzymatic, each of which has advantages and limitations. Although enzyme-based approaches possess high specificity, their stability and expensive preparation methods can be limitations. Contrary to the enzyme-based methods, enzyme-free approaches provide more sensitive probes for hydrogen peroxide detection. It seems that a combination of an aptamer with MSM could improve the specificity of the sensor for hydrogen peroxide detection. We believe that biocompatible silica-based materials (i.e. KCC-1, MSM, etc.) could be used in the future for the detection of hydrogen peroxide.

8. Amino acids and enzymes biosensing

Amino acids are important components in cells and tissues, that play a role in a wide variety of physiological reactions and biological processes [31]. Proteases are also used in various types of therapy, such as immune regulation, oncology, viral and infectious diseases [135]. Therefore, a change in protease concentration may be involved in the progression of some diseases [136].

Recently, a variety of fluorescent probes have been developed as a simple and direct assay based on chemical reactions between the probe and the target for the detection of biomolecules [137–139]. Li et al. [31] developed a ratiometric fluorescent probe using a 2,5-bis (benzo[d]thiazol-2-yl) (BTP) phenol scaffold for the real-time detection of cysteine (Cys) in human serum. This sensor relied on an excited state intramolecular proton transfer (ESIPT) mechanism, and could detect Cys as low as 0.38 μM. Moreover, this platform could be used for the measurement of Cys residues in BSA. As the main disadvantage, the sensitivity of the probe is limited and cannot cover the biological concentrations of Cys.

To increase the sensitivity for Cys determination, a scaffold combining AuNCs and CoO was synthesized by Nambiar et al. [32]. These scaffold naonoclusters showed a large number of available binding sites and could be used in electrocatalysis studies. They exploited a polycrystalline gold electrode based on a hybrid AuNC–CoO scaffold for the detection of Cys at a sub-nanomolar concentration. The electrochemical sensor exhibited excellent electrocatalytic activity for sensing of Cys within a dynamic range of 0.1 nM–1.0 μM and a low LOD of 16 pM. Accordingly, the highly sensitive hybrid film electrode could be used for the detection of Cys in clinical studies. The sensitivity of the scaffold was due to the incorporation of metal atoms, which resulted in a high current and a good response to the analyte.

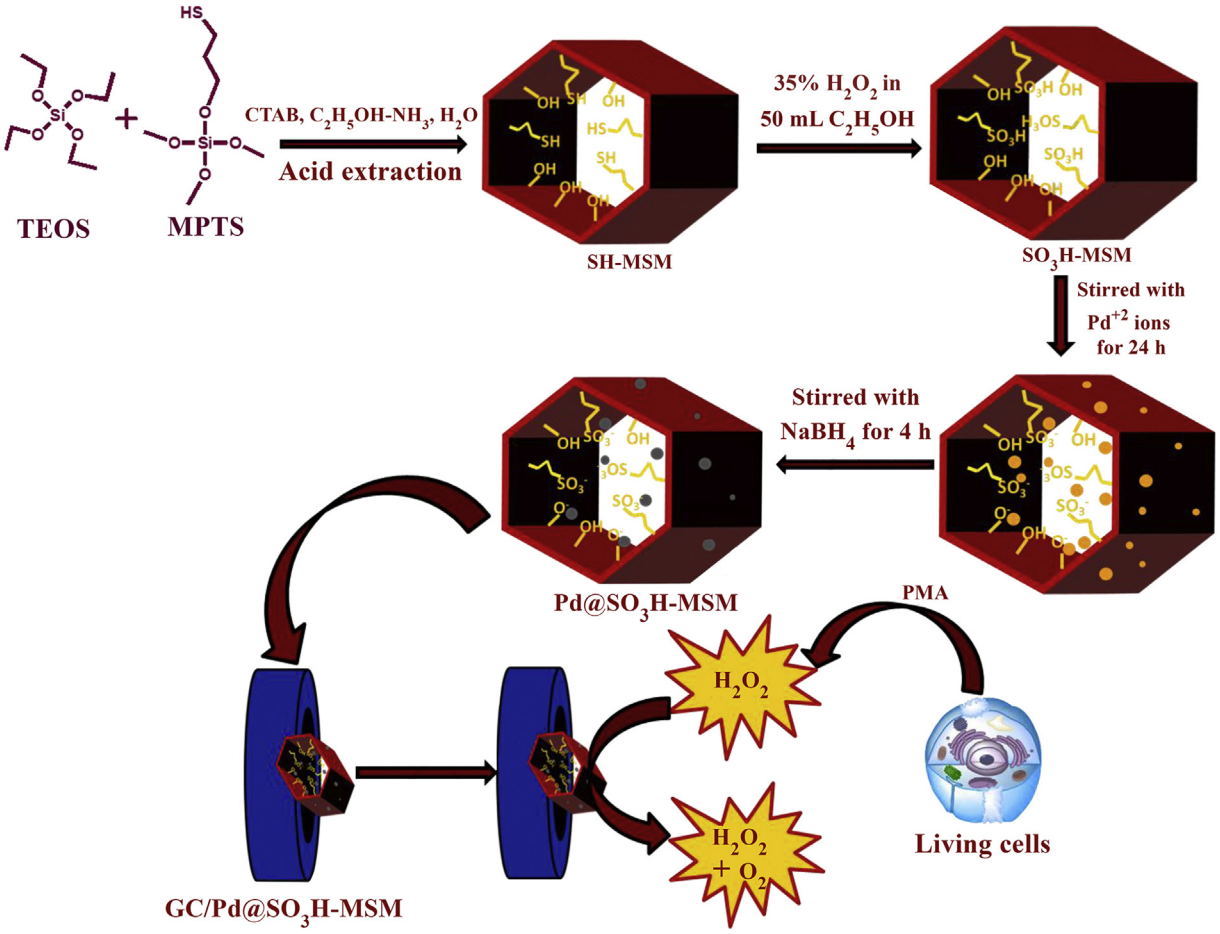

Fig. 7. Schematic representation of synthesis of GC/$Pd@SO_3H$-MSM and use as electrochemical GCE biosensor for detection of H_2O_2. (Reprinted (adapted) with permission from Ref. [27]. Copyright (2020) American Chemical Society).

Recently, porous cellulose nanocrystals (CNC) modified by poly(vinyl alcohol) (PVA) nanocomposites were described as a new type of scaffold for the detection of trypsin. Schyrr et al. [140] modified CNC/PVA with 2-(acryloxy)ethyl (3-isocyanato-4-methylphenyl) carbamate (HEA-TDI) and fluorescein (Fig. 8). Using a FRET mechanism, trypsin was determined at the 250 μg/mL level in wound fluid. In addition, Algar et al. [141] utilized a FRET mechanism with fluorescent dye labeled QDs (as a scaffold) to measure the protease activity of trypsin and chymotrypsin. This sensor could be used in wound healing studies to assess the degree of inflammation. Although both of the reported approaches for trypsin detection sufferred from low sensitivity, it is still of great importance to detect trypsin in wounded tissue.

While limited scaffold materials have been used for the detection of amino acids and enzymes employing electrochemical and fluorescence responses, none of the reported assays have yet been

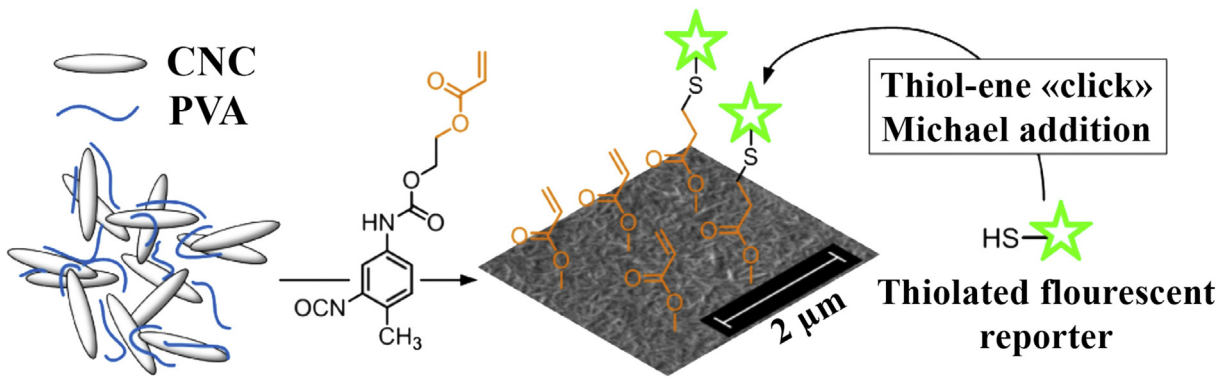

Fig. 8. Schematic illustration of cellulose nanocrystals (CNC)/poly(vinyl alcohol) (PVA) nanocomposite for the detection of proteases. CNC/PVA nanocomposite (with 25–75 nm thickness) was deposited using a dip-coating approach. (Reprinted (adapted) with permission from Ref. [140]. Copyright (2020) American Chemical Society).

approved as a reliable approach for clinical application. The safety of QDs and metal-based materials is still controversial because of concerns about toxicity and stability.

9. Conclusions

The reliable and rapid detection of biomarkers is an important goal of the whole biomedical community. Some of the traditionally employed approaches have suffered from low-sensitivity, time-consuming procedures, and non-specific responses. However, new advanced materials can provide benefits not only for the detection of biomarkers, but also in other fields that require an enhanced specific surface. Scaffolds are one type of advanced materials with a 3D structure, which have been extensively used in drug delivery and tissue engineering. However, recently, there has been an increasing interest to use scaffold materials (alone or hybrid) in the biomedical sensing of various analytes. In the present review, we have covered the biomedical applications of scaffold materials, concentrating on the detection and quantification of various bio-analytes. The extraordinary characteristics of these scaffolds, such as exceptional electroactivity and favorable spectroscopic properties, along with the three dimensional structure of the scaffold materials can overcome some of the limitations of currently employed approaches for the detection of analytes.

Five main classes of nanomaterials have been used in the fabrication of these scaffold platforms for the determination of analytes: (a) carbon-based materials, i.e. CDs, MWCNT, and graphene, which show high fluorescence QYs; (b) gold-based nanoparticles (AuNPs, AuNFs, AuNRs, and AuNTs) which possess excellent fluorescence quenching ability; (c) MOFs, which exhibit favorable electrical conductivity; (d) MCM and TiO_2, which are porous materials with good selectivity; and (e) organic molecules which can be self-assembled on the various scaffolds with tunable physicochemical properties for the simultaneous detection of multiplexed analytes.

A wide diversity of nanoparticles have been used for the recognition of various types of cancer biomarkers, however, CD/MOF-based sensors [72] showed the best performance for HER2 detection. While for the determination of other analytes, gold-based nanoparticles were more effective. Although, there are as yet no standard producers that can be recommended for use in clinical investigations, many of the reported methods have the potential to be used for *in situ* analysis of patient samples. However, before this step can occur, many more *ex vivo* studies should be conducted to evaluate their possible toxicity and confirm their reliability.

Notably, the fabrication of implantable platforms for continuous detection of biomarkers in living human subjects is an important goal in personalized medicine. Generally, natural scaffolds with good biocompatibility may be more rapidly translated into clinical applications after further in-depth study of their toxicity. Scaffold-based materials could be applied in 3D cell culture methods as a precursor to *in vivo* experiments for the assay of different biomarkers. The application of 3D scaffold materials offer scientists a possibility to more closely mimic the process occurring *in vivo*.

Future trends in scaffold-based materials for biomedical sensing will likely be focused on the following goals. Firstly, more reliable and stable implantable devices can be designed for the continuous detection of biomarkers. Secondly, some natural scaffolds (such as chitosan) can be incorporated into biosensors to enhance their safety and performance. Thirdly, scaffold-based materials could be incorporated in the development of wearable devices for real-time and *in-situ* detection of biomarkers either in healthy individuals, or for monitoring disease progression and response to therapy. Surprisingly, scaffold-based materials have not been employed in the design of wearable sensors up to the present time. Lastly, by employing new functionalization approaches (such as improved molecules for targeted detection or recognition), the LOD, the dynamic range, and the specificity of the platforms will be improved, and may even reach the single molecule detection level.

Declaration of competing interest

The authors declare the following financial interests/personal relationships which may be considered as potential competing interests:

MRH declares the following potential conflicts of interest. Scientific Advisory Boards: Transdermal Cap Inc, Cleveland, OH; BeWell Global Inc, Wan Chai, Hong Kong; Hologenix Inc. Santa Monica, CA; LumiThera Inc, Poulsbo, WA; Vielight, Toronto, Canada; Bright Photomedicine, Sao Paulo, Brazil; Quantum Dynamics LLC, Cambridge, MA; Global Photon Inc, Bee Cave, TX; Medical Coherence, Boston MA; NeuroThera, Newark DE; JOOVV Inc, Minneapolis-St. Paul MN; AIRx Medical, Pleasanton CA; FIR Industries, Inc. Ramsey, NJ; UVLRx Therapeutics, Oldsmar, FL; Ultralux UV Inc, Lansing MI; Illumiheal & Petthera, Shoreline, WA; MB Lasertherapy, Houston, TX; ARRC LED, San Clemente, CA; Varuna Biomedical Corp. Incline Village, NV; Niraxx Light Therapeutics, Inc, Boston, MA. Consulting; Lexington Int, Boca Raton, FL; USHIO Corp, Japan; Merck KGaA, Darmstadt, Germany; Philips Electronics Nederland B.V. Eindhoven, Netherlands; Johnson & Johnson Inc, Philadelphia, PA; Sanofi-Aventis Deutschland GmbH, Frankfurt am Main, Germany. Stockholdings: Global Photon Inc, Bee Cave, TX; Mitonix, Newark, DE.

The other authors report no potential conflicts of interest.

Acknowledgements

This Research was supported by Pharmaceutical Analysis Research Center, Tabriz University of Medical Sciences. MRH was supported by US NIH Grants R01AI050875 and R21AI121700.

References

[1] S. Lee, H. Huang, M. Zelen, Early detection of disease and scheduling of screening examinations, Stat. Methods Med. Res. 13 (2004) 443–456. https://doi.org/10.1191/0962280204sm377ra.

[2] J. Shu, D. Tang, Recent advances in photoelectrochemical sensing: from engineered photoactive materials to sensing devices and detection modes, Anal. Chem. 92 (2020) 363–377. https://doi.org/10.1021/acs.analchem.9b04199.

[3] R. Zeng, W. Wang, M. Chen, Q. Wan, C. Wang, D. Knopp, D. Tang, CRISPR-Cas12a-driven MXene-PEDOT:PSS piezoresistive wireless biosensor, Nanomater. Energy 82 (2021) 105711. https://doi.org/10.1016/j.nanoen.2020.105711.

[4] R. Ng, R. Zang, K.K. Yang, N. Liu, S.-T. Yang, Three-dimensional fibrous scaffolds with microstructures and nanotextures for tissue engineering, RSC Adv. 2 (2012) 10110–10124. https://doi.org/10.1039/c2ra21085a.

[5] L. Yang, Orthopedic nanoceramics, in: Nanotechnology-Enhanced Orthop. Mater, Woodhead Publishing, Oxford, 2015, pp. 49–75. https://doi.org/10.1016/B978-0-85709-844-3.00003-3.

[6] N. Tschammer, Chapter twenty-five - virally encoded G protein-coupled receptors: overlooked therapeutic opportunities?, in: M.C.B.T.-A.R. in M.C. Desai (Editor), Annu. Rep. Med. Chem., Academic Press, 2012, pp. 379–392. https://doi.org/10.1016/B978-0-12-396492-2.00025-4.

[7] S.L. McGovern, Promiscuous ligands, in: Comprehensive Medicinal Chemistry II, Elsevier, Oxford, 2007, pp. 737–752. https://doi.org/10.1016/B0-08-045044-X/00053-5.

[8] X. Huang, J.Z. Williams, R. Chang, Z. Li, C.E. Burnett, R. Hernandez-Lopez, I. Setiady, E. Gai, D.M. Patterson, W. Yu, K.T. Roybal, W.A. Lim, T.A. Desai, DNA scaffolds enable efficient and tunable functionalization of biomaterials for immune cell modulation, Nat. Nanotechnol. 16 (2021) 214–223. https://doi.org/10.1038/s41565-020-00813-z.

[9] R. Pasricha, D. Sachdev, in: M. Ramalingam, S.B.T.-N.C., B.A. Ramakrishna (Editors), 7 - biological characterization of nanofiber composites, Woodhead Publishing, 2017, pp. 157–196. https://doi.org/10.1016/B978-0-08-100173-8.00007-7.

[10] B. Dhandayuthapani, Y. Yoshida, T. Maekawa, D.S. Kumar, Polymeric scaffolds in tissue engineering application: a review, Int. J. Polym. Sci. (2011) 290602. https://doi.org/10.1155/2011/290602, 2011.

[11] M. Yazdimamaghani, M. Razavi, D. Vashaee, K. Moharamzadeh, A.R. Boccaccini, L. Tayebi, Porous magnesium-based scaffolds for tissue engineering, Mater. Sci. Eng. C 71 (2017) 1253–1266. https://doi.org/10.1016/j.msec.2016.11.027.
[12] X. Wang, Y. Li, J. Xiong, P.D. Hodgson, C. Wen, Porous TiNbZr alloy scaffolds for biomedical applications, Acta Biomater. 5 (2009) 3616–3624. https://doi.org/10.1016/j.actbio.2009.06.002.
[13] G. Manivasagam, A. Reddy, D. Sen, S. Nayak, M.T. Mathew, A. Rajamanikam, in: R.B.T.-E. of B.E. Narayan (Editor), Dentistry: Restorative and Regenerative Approaches, Elsevier, Oxford, 2019, pp. 332–347. https://doi.org/10.1016/B978-0-12-801238-3.11017-7.
[14] Q.L. Loh, C. Choong, Three-dimensional scaffolds for tissue engineering applications: role of porosity and pore size, Tissue Eng. B Rev. 19 (2013) 485–502. https://doi.org/10.1089/ten.teb.2012.0437.
[15] M.P. Nikolova, M.S. Chavali, Recent advances in biomaterials for 3D scaffolds: a review, Bioact. Mater. 4 (2019) 271–292. https://doi.org/10.1016/j.bioactmat.2019.10.005.
[16] F.J. O'Brien, Biomaterials & scaffolds for tissue engineering, Mater. Today 14 (2011) 88–95. https://doi.org/10.1016/S1369-7021(11)70058-X.
[17] P. Deb, A.B. Deoghare, A. Borah, E. Barua, S. Das Lala, Scaffold development using biomaterials: a review, Mater. Today Proc. 5 (2018) 12909–12919. https://doi.org/10.1016/j.matpr.2018.02.276.
[18] A. Eltom, G. Zhong, A. Muhammad, Scaffold techniques and designs in tissue engineering functions and purposes: a review, Ann. Mater. Sci. Eng. (2019). https://doi.org/10.1155/2019/3429527, 2019.
[19] J.D. Kretlow, L. Klouda, A.G. Mikos, Injectable matrices and scaffolds for drug delivery in tissue engineering, Adv. Drug Deliv. Rev. 59 (2007) 263–273. https://doi.org/10.1016/j.addr.2007.03.013.
[20] L. Huang, J. Chen, Z. Yu, D. Tang, Self-powered temperature sensor with seebeck effect transduction for photothermal–thermoelectric coupled immunoassay, Anal. Chem. 92 (2020) 2809–2814. https://doi.org/10.1021/acs.analchem.9b05218.
[21] M.K. Balaconis, Y. Luo, H.A. Clark, Glucose-sensitive nanofiber scaffolds with an improved sensing design for physiological conditions, Analyst 140 (2015) 716–723. https://doi.org/10.1039/c4an01775g.
[22] N.S.K. Gowthaman, M.A. Raj, S.A. John, Nitrogen-doped graphene as a robust scaffold for the homogeneous deposition of copper nanostructures: a nonenzymatic disposable glucose sensor, ACS Sustain. Chem. Eng. 5 (2017) 1648–1658. https://doi.org/10.1021/acssuschemeng.6b02390.
[23] M.J. Young, B. Yu, T.J. Koob, Y. Moussy, F. Moussy, A novel porous collagen scaffold around an implantable biosensor for improving biocompatibility. I. In vitro/in vivo stability of the scaffold and in vitro sensitivity of the glucose sensor with scaffold, J. Biomed. Mater. Res. - Part A. 87 (2008) 136–146. https://doi.org/10.1002/jbm.a.31756.
[24] F. Su, S. Zhang, H. Ji, H. Zhao, J.Y. Tian, C. Sen Liu, Z. Zhang, S. Fang, X. Zhu, M. Du, Two-dimensional zirconium-based metal-organic framework nanosheet composites embedded with Au nanoclusters: a highly sensitive electrochemical aptasensor toward detecting cocaine, ACS Sens. 2 (2017) 998–1005. https://doi.org/10.1021/acssensors.7b00268.
[25] M. Oroval, M. Coronado-Puchau, J. Langer, M.N. Sanz-Ortiz, Á. Ribes, E. Aznar, C. Coll, M.D. Marcos, F. Sancenón, L.M. Liz-Marzán, R. Martínez-Máñez, Surface enhanced Raman scattering and gated materials for sensing applications: the ultrasensitive detection of mycoplasma and cocaine, Chem. Eur J. 22 (2016) 13488–13495. https://doi.org/10.1002/chem.201602457.
[26] N.S.K. Gowthaman, H.N. Lim, S. Shankar, Electrochemical scaffold based on silver phosphate nanoparticles for the quantification of acetaminophen in body fluids and pharmaceutical formulations, ACS Appl. Nano Mater. (2020). https://doi.org/10.1021/acsanm.9b01959.
[27] R. Gupta, P. Singh, V. Ganesan, B. Koch, P.K. Rastogi, D.K. Yadav, P.K. Sonkar, Palladium nanoparticles supported on mesoporous silica microspheres for enzyme-free amperometric detection of H2O2 released from living cells, Sensor. Actuator. B Chem. 276 (2018) 517–525. https://doi.org/10.1016/j.snb.2018.08.148.
[28] S. Bin He, G.W. Wu, H.H. Deng, A.L. Liu, X.H. Lin, X.H. Xia, W. Chen, Choline and acetylcholine detection based on peroxidase-like activity and protein antifouling property of platinum nanoparticles in bovine serum albumin scaffold, Biosens. Bioelectron. 62 (2014) 331–336. https://doi.org/10.1016/j.bios.2014.07.005.
[29] K.S. Hettie, T.E. Glass, Coumarin-3-aldehyde as a scaffold for the design of tunable PET-modulated fluorescent sensors for neurotransmitters, Chem. Eur J. 20 (2014) 17488–17499. https://doi.org/10.1002/chem.201403128.
[30] M.L. Cortez, M. Ceolín, O. Azzaroni, F. Battaglini, Electrochemical sensing platform based on polyelectrolyte–surfactant supramolecular assemblies incorporating carbon nanotubes, Anal. Chem. 83 (2011) 8011–8018. https://doi.org/10.1021/ac202213t.
[31] M. Li, K. Zheng, H. Chen, X. Liu, S. Xiao, J. Yan, X. Tan, N. Zhang, A novel 2,5-bis(benzo[d]thiazol-2-yl)phenol scaffold-based ratiometric fluorescent probe for sensing cysteine in aqueous solution and serum, Spectrochim. Acta Part A Mol. Biomol. Spectrosc. 217 (2019) 1–7. https://doi.org/10.1016/j.saa.2019.03.033.
[32] S.R. Nambiar, K.P. Prathish, G. Karthik, T.P. Rao, Hybrid gold atomic cluster-cobalt oxide scaffolds for dual tandem electrocatalytic sensing of cysteine, Biosens. Bioelectron. 26 (2011) 3920–3926. https://doi.org/10.1016/j.bios.2011.03.011.
[33] Y. Cai, Y. Jiang, L. Feng, Y. Hua, H. Liu, C. Fan, M. Yin, S. Li, X. Lv, H. Wang, Q-graphene-scaffolded covalent organic frameworks as fluorescent probes and sorbents for the fluorimetry and removal of copper ions, Anal. Chim. Acta 1057 (2019) 88–97. https://doi.org/10.1016/j.aca.2018.12.054.
[34] P. Kamoun, Mental retardation in Down syndrome: a hydrogen sulfide hpothesis, Med. Hypotheses 57 (2001) 389–392. https://doi.org/10.1054/mehy.2001.1377.
[35] WHO, Infectious Diseases Kill over 17 Million People a Year: WHO Warns of Global Crisis (n.d.), https://www.who.int/news/item/01-01-1996-infectious-diseases-kill-over-17-million-people-a-year-who-warns-of-global-crisis. (Accessed 14 December 2020).
[36] WHO, WHO Coronavirus Disease, (COVID-19) Dashboard (n.d.), https://covid19.who.int/. (Accessed 16 December 2020).
[37] J. Jiao, C. Duan, L. Xue, Y. Liu, W. Sun, Y. Xiang, DNA nanoscaffold-based SARS-CoV-2 detection for COVID-19 diagnosis, Biosens, Bioelectron 167 (2020) 112479. https://doi.org/10.1016/j.bios.2020.112479.
[38] M.I. Setyawati, R.V. Kutty, C.Y. Tay, X. Yuan, J. Xie, D.T. Leong, Novel theranostic DNA nanoscaffolds for the simultaneous detection and killing of escherichia coli and staphylococcus aureus, ACS Appl. Mater. Interfaces 6 (2014) 21822–21831. https://doi.org/10.1021/am502591c.
[39] M. Liu, Q. Zhang, J.D. Brennan, Y. Li, Graphene-DNAzyme-based fluorescent biosensor for Escherichia coli detection, MRS Commun 8 (2018) 687–694. https://doi.org/10.1557/mrc.2018.97.
[40] Y. Xu, H. Wang, C. Luan, Y. Liu, B. Chen, Y. Zhao, Aptamer-based hydrogel barcodes for the capture and detection of multiple types of pathogenic bacteria, Biosens. Bioelectron. 100 (2018) 404–410. https://doi.org/10.1016/j.bios.2017.09.032.
[41] N. Tawil, E. Sacher, E. Boulais, R. Mandeville, M. Meunier, X-ray photoelectron spectroscopic and transmission electron microscopic characterizations of bacteriophage-nanoparticle complexes for pathogen detection, J. Phys. Chem. C 117 (2013) 20656–20665. https://doi.org/10.1021/jp406148h.
[42] P. Zhang, H. Liu, X. Li, S. Ma, S. Men, H. Wei, J. Cui, H. Wang, A label-free fluorescent direct detection of live Salmonella typhimurium using cascade triple trigger sequences-regenerated strand displacement amplification and hairpin template-generated-scaffolded silver nanoclusters, Biosens. Bioelectron. 87 (2017) 1044–1049. https://doi.org/10.1016/j.bios.2016.09.037.
[43] A. Mobed, M. Hasanzadeh, P. Babaie, M. Aghazadeh, A. Mokhtarzadeh, M.A. Rezaee, Cetyltrimethyl ammonium bromide modified gold nanostructure supported by chitosan as a novel scaffold for immobilization of DNA and ultra-sensitive bioassay of Legionella pneumophila, Microchem. J. 149 (2019) 103961. https://doi.org/10.1016/j.microc.2019.05.061.
[44] D. Martínez-Matamoros, S. Castro-García, M. Balado, A. Matamoros-Veloza, M.A. Camargo-Valero, O. Cespedes, J. Rodríguez, M.L. Lemos, C. Jiménez, Preparation of functionalized magnetic nanoparticles conjugated with feroxamine and their evaluation for pathogen detection, RSC Adv. 9 (2019) 13533–13542. https://doi.org/10.1039/c8ra10440a.
[45] WHO, Promoting Cancer Early Diagnosis (n.d.), https://www.who.int/activities/promoting-cancer-early-diagnosis. (Accessed 3 January 2021).
[46] N. Goossens, S. Nakagawa, X. Sun, Y. Hoshida, Cancer biomarker discovery and validation, Transl. Cancer Res. 4 (2015) 256–269. https://doi.org/10.3978/j.issn.2218-676X.2015.06.04.
[47] K. Zhang, S. Lv, Q. Zhou, D. Tang, CoOOH nanosheets-coated g-C3N4/CuInS2 nanohybrids for photoelectrochemical biosensor of carcinoembryonic antigen coupling hybridization chain reaction with etching reaction, Sensor. Actuator. B Chem. 307 (2020) 127631. https://doi.org/10.1016/j.snb.2019.127631.
[48] Z. Yu, G. Cai, X. Liu, D. Tang, Pressure-based biosensor integrated with a flexible pressure sensor and an electrochromic device for visual detection, Anal. Chem. 93 (2021) 2916–2925. https://doi.org/10.1021/acs.analchem.0c04501.
[49] C. Magi-Galluzzi, Prostate cancer: diagnostic criteria and role of immunohistochemistry, Mod. Pathol. 31 (2018) S12. https://doi.org/10.1038/modpathol.2017.139.
[50] H. Brunnström, A. Johansson, S. Westbom-Fremer, M. Backman, D. Djureinovic, A. Patthey, M. Isaksson-Mettävainio, M. Gulyas, P. Micke, PD-L1 immunohistochemistry in clinical diagnostics of lung cancer: inter-pathologist variability is higher than assay variability, Mod. Pathol. 30 (2017) 1411. https://doi.org/10.1038/modpathol.2017.59.
[51] L.H. Trümper, B. Bürger, F. von Bonin, A. Hintze, G. von Blohn, M. Pfreundschuh, H. Daus, Diagnosis of pancreatic adenocarcinoma by polymerase chain reaction from pancreatic secretions, Br. J. Canc. 70 (1994) 278. https://doi.org/10.1038/bjc.1994.292.
[52] D.B. Husarik, H.C. Steinert, Single-photon emission computed tomography/computed tomographyfor sentinel node mapping in breast cancer, in: Semin. Nucl. Med., Elsevier, 2007, pp. 29–33.
[53] S. Song, F. Naeim, New applications of flow cytometry in cancer diagnosis and therapy, in: Cancer Diagnostics, Springer, 2004, pp. 199–232.
[54] L. Wu, X. Qu, Cancer biomarker detection: recent achievements and challenges, Chem. Soc. Rev. 44 (2015) 2963–2997. https://doi.org/10.1039/c4cs00370e.
[55] M. Hasanzadeh, S. Rahimi, E. Solhi, A. Mokhtarzadeh, N. Shadjou, J. Soleymani, S. Mahboob, Probing the antigen-antibody interaction towards ultrasensitive recognition of cancer biomarker in adenocarcinoma cell lysates using layer-by-layer assembled silver nano-cubics with porous structure on cysteamine caped GQDs, Microchem. J. 143 (2018) 379–393. https://doi.org/10.1016/j.microc.2018.08.028.

[56] S. Hassanpour, M. Hasanzadeh, A. Saadati, N. Shadjou, J. Soleymani, A. Jouyban, A novel paper based immunoassay of breast cancer specific carbohydrate (CA 15.3) using silver nanoparticles-reduced graphene oxide nano-ink technology: a new platform to construction of microfluidic paper-based analytical devices (μPADs) towards biomedica, Microchem. J. 146 (2019) 345–358. https://doi.org/10.1016/j.microc.2019.01.018.
[57] Z. Luo, L. Zhang, R. Zeng, L. Su, D. Tang, Near-infrared light-excited core–core–shell UCNP@Au@CdS upconversion nanospheres for ultrasensitive photoelectrochemical enzyme immunoassay, Anal. Chem. 90 (2018) 9568–9575. https://doi.org/10.1021/acs.analchem.8b02421.
[58] Z. Luo, Q. Qi, L. Zhang, R. Zeng, L. Su, D. Tang, Branched polyethylenimine-modified upconversion nanohybrid-mediated photoelectrochemical immunoassay with synergistic effect of dual-purpose copper ions, Anal. Chem. 91 (2019) 4149–4156. https://doi.org/10.1021/acs.analchem.8b05959.
[59] Z. Qiu, J. Shu, J. Liu, D. Tang, Dual-channel photoelectrochemical ratiometric aptasensor with up-converting nanocrystals using spatial-resolved technique on homemade 3D printed device, Anal. Chem. 91 (2019) 1260–1268. https://doi.org/10.1021/acs.analchem.8b05455.
[60] Z. Yu, Y. Tang, G. Cai, R. Ren, D. Tang, Paper electrode-based flexible pressure sensor for point-of-care immunoassay with digital multimeter, Anal. Chem. 91 (2019) 1222–1226. https://doi.org/10.1021/acs.analchem.8b04635.
[61] R. Aggarwal, G.R. Romero, V. Friedl, A. Weinstein, A. Foye, J. Huang, F. Feng, J.M. Stuart, E.J. Small, Clinical and genomic characterization of Low PSA Secretors: a unique subset of metastatic castration resistant prostate cancer, Prostate Cancer Prostatic Dis. (2020). https://doi.org/10.1038/s41391-020-0228-0.
[62] N. Lu, H. Pei, Z. Ge, C.R. Simmons, H. Yan, C. Fan, Charge transport within a three-dimensional dna nanostructure framework, J. Am. Chem. Soc. 134 (2012) 13148–13151. https://doi.org/10.1021/ja302447r.
[63] X. Chen, G. Zhou, P. Song, J. Wang, J. Gao, J. Lu, C. Fan, X. Zuo, Ultrasensitive electrochemical detection of prostate-specific antigen by using antibodies anchored on a DNA nanostructural scaffold, Anal. Chem. 86 (2014) 7337–7342. https://doi.org/10.1021/ac500054x.
[64] Q.M. Feng, Z. Zhou, M.X. Li, W. Zhao, J.J. Xu, H.Y. Chen, DNA tetrahedral scaffolds-based platform for the construction of electrochemiluminescence biosensor, Biosens. Bioelectron. 90 (2017) 251–257. https://doi.org/10.1016/j.bios.2016.11.060.
[65] J. Soleymani, M. Hasanzadeh, M.H. Somi, A. Jouyban, Differentiation and targeting of HT 29 cancer cells based on folate bioreceptor using cysteamine functionalized gold nano-leaf, Mater. Sci. Eng. C 107 (2020) 110320. https://doi.org/10.1016/j.msec.2019.110320.
[66] J. Soleymani, M. Hasanzadeh, N. Shadjou, M.H. Somi, A. Jouyban, Spectrofluorimetric cytosensing of colorectal cancer cells using terbium-doped dendritic fibrous nano-silica functionalized by folic acid, J. Pharmaceut. Biomed. Anal. 180 (2020) 113077. https://doi.org/10.1016/j.jpba.2019.113077.
[67] J. Soleymani, M. Hasanzadeh, M.H. Somi, N. Shadjou, A. Jouyban, Highly sensitive and specific cytosensing of HT 29 colorectal cancer cells using folic acid functionalized-KCC-1 nanoparticles, Biosens. Bioelectron. 132 (2019) 122–131. https://doi.org/10.1016/j.bios.2019.02.052.
[68] J. Soleymani, M. Hasanzadeh, M.H. Somi, N. Shadjou, A. Jouyban, Probing the specific binding of folic acid to folate receptor using amino-functionalized mesoporous silica nanoparticles for differentiation of MCF 7 tumoral cells from MCF 10A, Biosens. Bioelectron. 115 (2018) 61–69. https://doi.org/10.1016/j.bios.2018.05.025.
[69] H. Elnakat, M. Ratnam, Distribution, functionality and gene regulation of folate receptor isoforms: implications in targeted therapy, Adv. Drug Deliv. Rev. 56 (2004) 1067–1084.
[70] C.P. Leamon, P.S. Low, Folate-mediated targeting: from diagnostics to drug and gene delivery, Drug Discov. Today 6 (2001) 44–51. https://doi.org/10.1016/S1359-6446(00)01594-4.
[71] A.M. Fales, B.M. Crawford, T. Vo-Dinh, Folate receptor-targeted theranostic nanoconstruct for surface-enhanced Raman scattering imaging and photodynamic therapy, ACS Omega 1 (2016) 730–735. https://doi.org/10.1021/acsomega.6b00176.
[72] C. Gu, C. Guo, Z. Li, M. Wang, N. Zhou, L. He, Z. Zhang, M. Du, Bimetallic ZrHf-based metal-organic framework embedded with carbon dots: ultra-sensitive platform for early diagnosis of HER2 and HER2-overexpressed living cancer cells, Biosens, Bioelectron 134 (2019) 8–15. https://doi.org/10.1016/j.bios.2019.03.043.
[73] C. Guo, F. Su, Y. Song, B. Hu, M. Wang, L. He, D. Peng, Z. Zhang, Aptamer-templated silver nanoclusters embedded in zirconium metal-organic framework for bifunctional electrochemical and SPR aptasensors toward carcinoembryonic antigen, ACS Appl. Mater. Interfaces 9 (2017) 41188–41199. https://doi.org/10.1021/acsami.7b14952.
[74] S. Asadi, M. Jamali, H. Mohammadzadeh, Identification of carcinoma embryonic antigen release mechanism Carcinoembryonic Antigen (CEA) from the surface of colorectal cancer cells, Res. Rev. Insights. 1 (2017) 1–7. https://doi.org/10.15761/rri.1000109.
[75] N. Zhou, F. Su, C. Guo, L. He, Z. Jia, M. Wang, Q. Jia, Z. Zhang, S. Lu, Two-dimensional oriented growth of Zn-MOF-on-Zr-MOF architecture: a highly sensitive and selective platform for detecting cancer markers, Biosens. Bioelectron. 123 (2019) 51–58. https://doi.org/10.1016/j.bios.2018.09.079.
[76] C.S. Park, T.H. Ha, M. Kim, N. Raja, H. suk Yun, M.J. Sung, O.S. Kwon, H. Yoon, C.S. Lee, Fast and sensitive near-infrared fluorescent probes for ALP detection and 3d printed calcium phosphate scaffold imaging in vivo, Biosens. Bioelectron. 105 (2018) 151–158. https://doi.org/10.1016/j.bios.2018.01.018.
[77] W.X. Du, S.F. Duan, J.J. Chen, J.F. Huang, L.M. Yin, P.J. Tong, Serum bone-specific alkaline phosphatase as a biomarker for osseous metastases in patients with malignant carcinomas: a systematic review and meta-analysis, J. Canc. Res. Therapeut. 10 (2014) C140–C143. https://doi.org/10.4103/0973-1482.145842.
[78] Z. Chen, S.B. Cheng, P. Cao, Q.F. Qiu, Y. Chen, M. Xie, Y. Xu, W.H. Huang, Detection of exosomes by ZnO nanowires coated three-dimensional scaffold chip device, Biosens. Bioelectron. 122 (2018) 211–216. https://doi.org/10.1016/j.bios.2018.09.033.
[79] C. Xue, S. Zhang, C. Li, X. Yu, C. Ouyang, Y. Lu, Z.S. Wu, Y-shaped backbone-rigidified triangular DNA scaffold-directed stepwise movement of a DNAzyme walker for sensitive microRNA imaging within living cells, Anal. Chem. 91 (2019) 15678–15685. https://doi.org/10.1021/acs.analchem.9b03784.
[80] D. Wang, Y. Chai, Y. Yuan, R. Yuan, Precise regulation of enzyme cascade catalytic efficiency with DNA tetrahedron as scaffold for ultrasensitive electrochemical detection of DNA, Anal. Chem. 91 (2019) 3561–3566. https://doi.org/10.1021/acs.analchem.8b05407.
[81] J. Soleymani, M. Hasanzadeh, N. Shadjou, M.H. Somi, A. Jouyban, The role of nanomaterials on the cancer cells sensing based on folate receptor: analytical approach, TrAC Trends Anal. Chem. (Reference Ed.) 125 (2020) 115834. https://doi.org/10.1016/j.trac.2020.115834.
[82] M. Fani, M.-L. Tamma, G.P. Nicolas, E. Lasri, C. Medina, I. Raynal, M. Port, W.A. Weber, H.R. Maecke, In vivo imaging of folate receptor positive tumor xenografts using Novel 68Ga-NODAGA-folate conjugate, Mol. Pharm. 9 (2012) 1136–1145. https://doi.org/10.1021/mp200418f.
[83] H.S. Yoo, T.G. Park, Folate-receptor-targeted delivery of doxorubicin nano-aggregates stabilized by doxorubicin–PEG–folate conjugate, J. Contr. Release 100 (2004) 247–256. https://doi.org/10.1016/j.jconrel.2004.08.017.
[84] S. Nalbantoglu, H. Amri, Single-cell omics: strategies towards theranostic biomarker discovery along the continuum of premalignant to invasive disease in oncology, Single-Cell Omi, Appl. Biomed. Agric. 2 (2019) 105–128. https://doi.org/10.1016/B978-0-12-817532-3.00006-2.
[85] T. Yu, P.P. Dai, J.J. Xu, H.Y. Chen, Highly sensitive colorimetric cancer cell detection based on dual signal amplification, ACS Appl. Mater. Interfaces 8 (2016) 4434–4441. https://doi.org/10.1021/acsami.5b12117.
[86] R. Zeng, L. Zhang, Z. Luo, D. Tang, Palindromic fragment-mediated single-chain amplification: an innovative mode for photoelectrochemical bioassay, Anal. Chem. 91 (2019) 7835–7841. https://doi.org/10.1021/acs.analchem.9b01557.
[87] R. Zeng, Z. Luo, L. Su, L. Zhang, D. Tang, R. Niessner, D. Knopp, Palindromic molecular beacon based Z-scheme BiOCl-Au-CdS photoelectrochemical biodetection, Anal. Chem. 91 (2019) 2447–2454. https://doi.org/10.1021/acs.analchem.8b05265.
[88] A. Umar, A.A. Ibrahim, R. Kumar, T. Almas, P. Sandal, M.S. Al-Assiri, M.H. Mahnashi, B.Z. AlFarhan, S. Baskoutas, Fern shaped La2O3 nanostructures as potential scaffold for efficient hydroquinone chemical sensing application, Ceram. Int. 46 (2020) 5141–5148. https://doi.org/10.1016/j.ceramint.2019.10.258.
[89] R. Zeng, L. Zhang, L. Su, Z. Luo, Q. Zhou, D. Tang, Photoelectrochemical bioanalysis of antibiotics on rGO-Bi2WO6-Au based on branched hybridization chain reaction, Biosens. Bioelectron. 133 (2019) 100–106. https://doi.org/10.1016/j.bios.2019.02.067.
[90] R. Zeng, J. Tao, D. Tang, D. Knopp, J. Shu, X. Cao, Biometric-based tactile chemomechanical transduction: an adaptable strategy for portable bioassay, Nanomater. Energy 71 (2020) 104580. https://doi.org/10.1016/j.nanoen.2020.104580.
[91] S. Velmurugan, S. Palanisamy, T.C.-K. Yang, M. Gochoo, S.W. Chen, Ultrasonic assisted functionalization of MWCNT and synergistic electrocatalytic effect of nano-hydroxyapatite incorporated MWCNT-chitosan scaffolds for sensing of nitrofurantoin, Ultrason. Sonochem. 62 (2020) 104863. https://doi.org/10.1016/j.ultsonch.2019.104863.
[92] B.J.F. Swift, J.A. Shadish, C.A. DeForest, F. Baneyx, Streamlined synthesis and assembly of a hybrid sensing architecture with solid binding proteins and click chemistry, J. Am. Chem. Soc. 139 (2017) 3958–3961. https://doi.org/10.1021/jacs.7b00519.
[93] F. Tian, C. Wang, M. Tang, J. Li, X. Cheng, S. Zhang, D. Ji, Y. Huang, H. Li, The antibiotic chloramphenicol may be an effective new agent for inhibiting the growth of multiple myeloma, Oncotarget 7 (2016) 51934–51942. https://doi.org/10.18632/oncotarget.10623.
[94] S. Suelzu, A. Cossu, G. Pala, M. Portoghese, V. Columbanu, G. Sales, L. Solinas, L. Brazzi, Impact of different dosage of protamine on heparin reversal during off-pump coronary artery bypass: a clinical study, Hear, Lung Vessel 7 (2015) 238–245.
[95] B.F. Akl, G.M. Vargas, J. Neal, J. Robillard, P. Kelly, Clinical experience with the activated clotting time for the control of heparin and protamine therapy during cardiopulmonary bypass, J. Thorac. Cardiovasc. Surg. 79 (1980) 97–102. https://doi.org/10.1016/S0022-5223(19)38010-9.
[96] R.S. Dey, C.R. Raj, Polyelectrolyte-functionalized gold nanoparticle scaffold for the sensing of heparin and protamine in serum, Chem. Asian J. 7 (2012) 417–424. https://doi.org/10.1002/asia.201100686.
[97] S. Wang, Z. Li, F. Duan, B. Hu, L. He, M. Wang, N. Zhou, Q. Jia, Z. Zhang, Bimetallic cerium/copper organic framework-derived cerium and copper oxides embedded by mesoporous carbon: label-free aptasensor for

ultrasensitive tobramycin detection, Anal. Chim. Acta 1047 (2019) 150–162. https://doi.org/10.1016/j.aca.2018.09.064.
[98] S. Soylemez, B. Yoon, L. Toppare, T.M. Swager, Quaternized polymer-single-walled carbon nanotube scaffolds for a chemiresistive glucose sensor, ACS Sens. 2 (2017) 1123–1127. https://doi.org/10.1021/acssensors.7b00323.
[99] R.S. Dey, R.K. Bera, C.R. Raj, Nanomaterial-based functional scaffolds for amperometric sensing of bioanalytes, Anal. Bioanal. Chem. 405 (2013) 3431–3448. https://doi.org/10.1007/s00216-012-6606-2.
[100] A.K. Rines, K. Sharabi, C.D.J. Tavares, P. Puigserver, Targeting hepatic glucose metabolism in the treatment of type 2 diabetes, Nat. Rev. Drug Discov. 15 (2016) 786–804. https://doi.org/10.1038/nrd.2016.151.
[101] Q. Qian, Q. Hu, L. Li, P. Shi, J. Zhou, J. Kong, X. Zhang, G. Sun, W. Huang, Sensitive fiber microelectrode made of nickel hydroxide nanosheets embedded in highly-aligned carbon nanotube scaffold for nonenzymatic glucose determination, Sensor. Actuator. B Chem. 257 (2018) 23–28. https://doi.org/10.1016/j.snb.2017.10.110.
[102] A. Umar, R. Ahmad, A. Al-Hajry, S.H. Kim, M.E. Abaker, Y.B. Hahn, Spruce branched α-Fe2O3 nanostructures as potential scaffolds for a highly sensitive and selective glucose biosensor, New J. Chem. 38 (2014) 5873–5879. https://doi.org/10.1039/c4nj01148a.
[103] A. Zhao, Z. Zhang, P. Zhang, S. Xiao, L. Wang, Y. Dong, H. Yuan, P. Li, Y. Sun, X. Jiang, F. Xiao, 3D nanoporous gold scaffold supported on graphene paper: freestanding and flexible electrode with high loading of ultrafine PtCo alloy nanoparticles for electrochemical glucose sensing, Anal. Chim. Acta 938 (2016) 63–71. https://doi.org/10.1016/j.aca.2016.08.013.
[104] Z. Gao, Y. Lin, Y. He, D. Tang, Enzyme-free amperometric glucose sensor using a glassy carbon electrode modified with poly(vinyl butyral) incorporating a hybrid nanostructure composed of molybdenum disulfide and copper sulfide, Microchim. Acta. 184 (2017) 807–814. https://doi.org/10.1007/s00604-016-2061-7.
[105] Y.M. Ju, B. Yu, L. West, Y. Moussy, F. Moussy, A novel porous collagen scaffold around an implantable biosensor for improving biocompatibility. II. Long-term in vitro/in vivo sensitivity characteristics of sensors with NDGA- or GA-crosslinked collagen scaffolds, J. Biomed. Mater. Res. - Part A. 92 (2010) 650–658. https://doi.org/10.1002/jbm.a.32400.
[106] R. Ravichandran, J.G. Martinez, E.W.H. Jager, J. Phopase, A.P.F. Turner, Type i collagen-derived injectable conductive hydrogel scaffolds as glucose sensors, ACS Appl. Mater. Interfaces 10 (2018) 16244–16249. https://doi.org/10.1021/acsami.8b04091.
[107] R. Zeng, Z. Huang, Y. Wang, D. Tang, Enzyme-encapsulated DNA hydrogel for highly efficient electrochemical sensing glucose, ChemElectroChem 7 (2020) 1537–1541. https://doi.org/10.1002/celc.202000105.
[108] Y. Onuki, U. Bhardwaj, F. Papadimitrakopoulos, D.J. Burgess, A review of the biocompatibility of implantable devices: current challenges to overcome foreign body response, J. Diabetes Sci. Technol. 2 (2008) 1003–1015. https://doi.org/10.1177/193229680800200610.
[109] X. Xie, W. Zhang, A. Abbaspourrad, J. Ahn, A. Bader, S. Bose, A. Vegas, J. Lin, J. Tao, T. Hang, H. Lee, N. Iverson, G. Bisker, L. Li, M.S. Strano, D.A. Weitz, D.G. Anderson, Microfluidic fabrication of colloidal nanomaterials-encapsulated microcapsules for biomolecular sensing, Nano Lett. 17 (2017) 2015–2020. https://doi.org/10.1021/acs.nanolett.7b00026.
[110] M. Grätzel, Photoelectrochemical cells, Nature 414 (2001) 338–344. https://doi.org/10.1038/35104607.
[111] X. Liu, X. Huo, P. Liu, Y. Tang, J. Xu, X. Liu, Y. Zhou, Assembly of MoS2 nanosheet-TiO2 nanorod heterostructure as sensor scaffold for photo-electrochemical biosensing, Electrochim. Acta 242 (2017) 327–336. https://doi.org/10.1016/j.electacta.2017.05.037.
[112] B. Si, E. Song, Recent advances in the detection of neurotransmitters, Chemosensors 6 (2018) 1–24. https://doi.org/10.3390/chemosensors6010001.
[113] A. Liu, I. Honma, H. Zhou, Amperometric biosensor based on tyrosinase-conjugated polysacchride hybrid film: selective determination of nano-molar neurotransmitters metabolite of 3,4-dihydroxyphenylacetic acid (DOPAC) in biological fluid, Biosens. Bioelectron. 21 (2005) 809–816. https://doi.org/10.1016/j.bios.2005.03.005.
[114] J. Soleymani, Advanced materials for optical sensing and biosensing of neurotransmitters, TrAC Trends Anal. Chem. (Reference Ed.) 72 (2015) 27–44. https://doi.org/10.1016/j.trac.2015.03.017.
[115] B. Ma, S. Wu, F. Zeng, Y. Luo, J. Zhao, Z. Tong, Nanosized diblock copolymer micelles as a scaffold for constructing a ratiometric fluorescent sensor for metal ion detection in aqueous media, Nanotechnology 21 (2010). https://doi.org/10.1088/0957-4484/21/19/195501.
[116] B. Halliwell, J.M.C.B.T.-M. in E. Gutteridge, Role of free radicals and catalytic metal ions in human disease: an overview, in: Oxyg. Radicals Biol. Syst. Part B Oxyg. Radicals Antioxidants, Academic Press, 1990, pp. 1–85. https://doi.org/10.1016/0076-6879(90)86093-B.
[117] S.A. El-Safty, M.A. Shenashen, A. Shahat, Tailor-made micro-object optical sensor based on mesoporous pellets for visual monitoring and removal of toxic metal ions from aqueous media, Small 9 (2013) 2288–2296. https://doi.org/10.1002/smll.201202407.
[118] T. Priya, N. Dhanalakshmi, S. Thennarasu, N. Thinakaran, A novel voltammetric sensor for the simultaneous detection of Cd2+ and Pb2+ using graphene oxide/κ-carrageenan/L-cysteine nanocomposite, Carbohydr. Polym. 182 (2018) 199–206. https://doi.org/10.1016/j.carbpol.2017.11.017.
[119] Y. Liu, X. Qu, Q. Guo, Q. Sun, X. Huang, QD-Biopolymer-TSPP assembly as efficient BiFRET sensor for ratiometric and visual detection of zinc ion, ACS Appl. Mater. Interfaces 9 (2017) 4725–4732. https://doi.org/10.1021/acsami.6b14972.
[120] M. Hagimori, T. Uto, N. Mizuyama, T. Temma, Y. Yamaguchi, Y. Tominaga, H. Saji, Fluorescence ON/OFF switching Zn2+ sensor based on pyridine-pyridone scaffold, Sensor. Actuator. B Chem. 181 (2013) 823–828. https://doi.org/10.1016/j.snb.2013.02.033.
[121] K. Komatsu, Y. Urano, H. Kojima, T. Nagano, Development of an iminocoumarin-based zinc sensor suitable for ratiometric fluorescence imaging of neuronal zinc, J. Am. Chem. Soc. 129 (2007) 13447–13454. https://doi.org/10.1021/ja072432g.
[122] R. Ren, G. Cai, Z. Yu, Y. Zeng, D. Tang, Metal-polydopamine framework: an innovative signal-generation tag for colorimetric immunoassay, Anal. Chem. 90 (2018) 11099–11105. https://doi.org/10.1021/acs.analchem.8b03538.
[123] Z. Gao, S. Lv, M. Xu, D. Tang, High-index {hk0} faceted platinum concave nanocubes with enhanced peroxidase-like activity for an ultrasensitive colorimetric immunoassay of the human prostate-specific antigen, Analyst 142 (2017) 911–917. https://doi.org/10.1039/C6AN02722A.
[124] W. Lai, Q. Wei, M. Xu, J. Zhuang, D. Tang, Enzyme-controlled dissolution of MnO2 nanoflakes with enzyme cascade amplification for colorimetric immunoassay, Biosens. Bioelectron. 89 (2017) 645–651. https://doi.org/10.1016/j.bios.2015.12.035.
[125] R. Ren, G. Cai, Z. Yu, D. Tang, Glucose-loaded liposomes for amplified colorimetric immunoassay of streptomycin based on enzyme-induced iron(II) chelation reaction with phenanthroline, Sensor. Actuator. B Chem. 265 (2018) 174–181. https://doi.org/10.1016/j.snb.2018.03.049.
[126] Z. Gao, Z. Qiu, M. Lu, J. Shu, D. Tang, Hybridization chain reaction-based colorimetric aptasensor of adenosine 5′-triphosphate on unmodified gold nanoparticles and two label-free hairpin probes, Biosens. Bioelectron. 89 (2017) 1006–1012. https://doi.org/10.1016/j.bios.2016.10.043.
[127] A.R. Ferhan, L. Guo, X. Zhou, P. Chen, S. Hong, D.H. Kim, Solid-phase colorimetric sensor based on gold nanoparticle-loaded polymer brushes: lead detection as a case study, Anal. Chem. 85 (2013) 4094–4099. https://doi.org/10.1021/ac4001817.
[128] H. Liu, L. Weng, C. Yang, A review on nanomaterial-based electrochemical sensors for H2O2, H2S and NO inside cells or released by cells, Microchim, Acta 184 (2017) 1267–1283. https://doi.org/10.1007/s00604-017-2179-2.
[129] P. Wu, Z. Cai, Y. Gao, H. Zhang, C. Cai, Enhancing the electrochemical reduction of hydrogen peroxide based on nitrogen-doped graphene for measurement of its releasing process from living cells, Chem. Commun. 47 (2011) 11327–11329. https://doi.org/10.1039/c1cc14419g.
[130] X. Liu, J. Zhang, S. Liu, Q. Zhang, X. Liu, D.K.Y. Wong, Gold nanoparticle encapsulated-tubular TIO2 nanocluster as a scaffold for development of thiolated enzyme biosensors, Anal. Chem. 85 (2013) 4350–4356. https://doi.org/10.1021/ac303420a.
[131] D. Lu, J. Cardiel, G. Cao, A.Q. Shen, Nanoporous scaffold with immobilized enzymes during flow-induced gelation for sensitive H2O2 biosensing, Adv. Mater. 22 (2010) 2809–2813. https://doi.org/10.1002/adma.201000189.
[132] S. Zong, Y. Cao, Y. Zhou, H. Ju, Zirconia nanoparticles enhanced grafted collagen tri-helix scaffold for unmediated biosensing of hydrogen peroxide, Langmuir 22 (2006) 8915–8919. https://doi.org/10.1021/la060930h.
[133] V. Mani, R. Devasenathipathy, S.M. Chen, S.F. Wang, P. Devi, Y. Tai, Electrodeposition of copper nanoparticles using pectin scaffold at graphene nanosheets for electrochemical sensing of glucose and hydrogen peroxide, Electrochim. Acta 176 (2015) 804–810. https://doi.org/10.1016/j.electacta.2015.07.098.
[134] Y. Zhang, J. Xiao, Q. Lv, L. Wang, X. Dong, M. Asif, J. Ren, W. He, Y. Sun, F. Xiao, S. Wang, In situ electrochemical sensing and real-time monitoring live cells based on freestanding nanohybrid paper electrode assembled from 3D functionalized graphene framework, ACS Appl. Mater. Interfaces 9 (2017) 38201–38210. https://doi.org/10.1021/acsami.7b08781.
[135] K.A. Mahmoud, S. Hrapovic, J.H.T. Luong, Picomolar detection of protease using peptide single walled carbon nanotube gold nanoparticle-modified electrode, ACS Nano 2 (2008) 1051–1057. https://doi.org/10.1021/nn8000774.
[136] C.J. Mu, D.A. LaVan, R.S. Langer, B.R. Zetter, Self-assembled gold nanoparticle molecular probes for detecting proteolytic activity in vivo, ACS Nano 4 (2010) 1511–1520. https://doi.org/10.1021/nn9017334.
[137] A. Jouyban, M. Shaghaghi, J.L. Manzoori, J. Soleymani, J. Vaez-Gharamaleki, Determination of methotrexate in biological fluids and a parenteral injection using terbium-sensitized method, Iran, J. Pharm. Res. 10 (2011) 695–704. https://doi.org/10.22037/IJPR.2011.990.
[138] J.L. Manzoori, M. Amjadi, J. Soleymani, E. Tamizi, A. Rezamand, A. Jouyban, Determination of deferiprone in urine and serum using a terbium-sensitized luminescence method, Luminescence 27 (2012) 268–273. https://doi.org/10.1002/bio.1344.
[139] J. Manzoori-Lashkar, M. Amjadi, J. Soleymani, E. Tamizi, V. Panahi-Azar, A. Jouyban, Development and validation of a terbium-sensitized luminescenceanalytical method for deferiprone, Iran, J. Pharm. Res. 11 (2012) 771–780. https://doi.org/10.22037/IJPR.2012.1124.
[140] B. Schyrr, S. Pasche, G. Voirin, C. Weder, Y.C. Simon, E.J. Foster, Biosensors based on porous cellulose nanocrystal-poly(vinyl alcohol) scaffolds, ACS Appl. Mater. Interfaces 6 (2014) 12674–12683. https://doi.org/10.1021/am502670u.
[141] W.R. Algar, M.G. Ancona, A.P. Malanoski, K. Susumu, I.L. Medintz, Assembly of a concentric förster resonance energy transfer relay on a quantum dot scaffold: characterization and application to multiplexed protease sensing, ACS Nano 6 (2012) 11044–11058. https://doi.org/10.1021/nn304736j.